AFRL-VA-WP-TR-2003-3071

SURVIVABILITY OF AFFORDABLE AIRCRAFT COMPOSITE STRUCTURES

Volume 1: Overview and Ballistic Impact Testing of Affordable Woven Carbon/Epoxy Composites

Dr. Mahesh V. Hosur and Dr. Shaik Jeelani

Tuskegee University
Center for Advanced Materials
Tuskegee, AL 36088

Dr. Uday K. Vaidya
The University of Alabama in Birmingham

Dr. Sylvanus Nwosu
University of Pittsburgh

Dr. Ajit D. Kelkar
North Carolina A&T State University

APRIL 2003

Final Report for 01 October 1999 – 01 March 2003

Approved for public release; distribution is unlimited.

STINFO FINAL REPORT

AIR VEHICLES DIRECTORATE
AIR FORCE RESEARCH LABORATORY
AIR FORCE MATERIEL COMMAND
WRIGHT-PATTERSON AIR FORCE BASE, OH 45433-7542

NOTICE

USING GOVERNMENT DRAWINGS, SPECIFICATIONS, OR OTHER DATA INCLUDED IN THIS DOCUMENT FOR ANY PURPOSE OTHER THAN GOVERNMENT PROCUREMENT DOES NOT IN ANY WAY OBLIGATE THE U.S. GOVERNMENT. THE FACT THAT THE GOVERNMENT FORMULATED OR SUPPLIED THE DRAWINGS, SPECIFICATIONS, OR OTHER DATA DOES NOT LICENSE THE HOLDER OR ANY OTHER PERSON OR CORPORATION; OR CONVEY AND RIGHTS OR PERMISSION TO MANUFACTURE, USE, OR SELL ANY PATENTED INVENTION THAT MAY RELATE TO THEM.

THIS REPORT HAS BEEN REVIEWED BY THE OFFICE OF PUBLIC AFFAIRS (ASC/PA) AND IS RELEASABLE TO THE NATIONAL TECHNICAL INFORMATION SERVICE (NTIS). AT NTIS, IT WILL BE AVAILABLE TO THE GENERAL PUBLIC, INCLUDING FOREIGN NATIONS.

THIS TECHNICAL REPORT HAS BEEN REVIEWED AND IS APPROVED FOR PUBLICATION.

/s/

ARNOLD H. MAYER
Project Engineer
Design and Analysis Methods Branch
Structures Division

/s/

MICHAEL L. ZEIGLER, Chief
Design and Analysis Methods Branch
Structures Division

/s/

DAVID M. PRATT, PhD
Technical Advisor
Structures Division

COPIES OF THIS REPORT SHOULD NOT BE RETURNED UNLESS RETURN IS REQUIRED BY SECURITY CONSIDERATIONS, CONTRACTUAL OBLIGATIONS, OR NOTICE ON A SPECIFIC DOCUMENT.

REPORT DOCUMENTATION PAGE

Form Approved
OMB No. 0704-0188

The public reporting burden for this collection of information is estimated to average 1 hour per response, including the time for reviewing instructions, searching existing data sources, searching existing data sources, gathering and maintaining the data needed, and completing and reviewing the collection of information. Send comments regarding this burden estimate or any other aspect of this collection of information, including suggestions for reducing this burden, to Department of Defense, Washington Headquarters Services, Directorate for Information Operations and Reports (0704-0188), 1215 Jefferson Davis Highway, Suite 1204, Arlington, VA 22202-4302. Respondents should be aware that notwithstanding any other provision of law, no person shall be subject to any penalty for failing to comply with a collection of information if it does not display a currently valid OMB control number. **PLEASE DO NOT RETURN YOUR FORM TO THE ABOVE ADDRESS**.

1. REPORT DATE *(DD-MM-YY)*	2. REPORT TYPE	3. DATES COVERED *(From - To)*
April 2003	Final	10/01/1999 – 03/01/2003

4. TITLE AND SUBTITLE
SURVIVABILITY OF AFFORDABLE AIRCRAFT COMPOSITE STRUCTURES
Volume 1: Overview and Ballistic Impact Testing of Affordable Woven Carbon/Epoxy Composites

5a. CONTRACT NUMBER
F33615-99-C-3608

5b. GRANT NUMBER

5c. PROGRAM ELEMENT NUMBER
62201F

6. AUTHOR(S)
Dr. Mahesh V. Hosur and Dr. Shaik Jeelani (Tuskegee University)
Dr. Uday K. Vaidya (The University of Alabama in Birmingham)
Dr. Sylvanus Nwosu (University of Pittsburgh)
Dr. Ajit D. Kelkar (North Carolina A&T State University)

5d. PROJECT NUMBER
2402

5e. TASK NUMBER
SA

5f. WORK UNIT NUMBER
AC

7. PERFORMING ORGANIZATION NAME(S) AND ADDRESS(ES)
Tuskegee University
Center for Advanced Materials
Tuskegee, AL 36088
The University of Alabama in Birmingham
University of Pittsburgh
North Carolina A&T State University

8. PERFORMING ORGANIZATION REPORT NUMBER

9. SPONSORING/MONITORING AGENCY NAME(S) AND ADDRESS(ES)
Air Vehicles Directorate
Air Force Research Laboratory
Air Force Materiel Command
Wright-Patterson Air Force Base, OH 45433-7542

10. SPONSORING/MONITORING AGENCY ACRONYM(S)
AFRL/VASD

11. SPONSORING/MONITORING AGENCY REPORT NUMBER(S)
AFRL-VA-WP-TR-2003-3071

12. DISTRIBUTION/AVAILABILITY STATEMENT
Approved for public release; distribution is unlimited.

13. SUPPLEMENTARY NOTES
This is volume 1 of three. See also AFRL-VA-WP-TR-2003-3072 and AFRL-VA-WP-TR-2003-3073. This report contains color.

14. ABSTRACT ***(Maximum 200 Words)***
Future aircraft technology enhancements (FATE) develop revolutionary technologies that will become the foundation for the next generation of war fighters. The structures thrust of the Air Vehicles Directorate further supports the Air Force need toward a composite affordability initiative (CAI). Affordability and survivability are keys to air and space vehicles for higher performance, longer life, and cost effectiveness. In the current research project, issues of CAI were addressed. The technical work carried out is presented in three volumes.
Volume 1 addresses the performance of carbon/epoxy composites that were manufactured using affordable vacuum assisted infusion molding (VARIM) process. Panels made of stitched/unstitched plain, satin, and twill weave of different thicknesses were subjected to high velocity impact loading using a gas-gun facility. Damage modes were evaluated through ultrasonic nondestructive evaluation (NDE). Effect of projectile geometry was studied. In all of the laminates, the damage was localized and was dominated by penetration rather than delamination. This resulted in laminates with lower damage size with increased residual mechanical properties as compared to the unidirectional laminates that are used in the current aircraft structures.

15. SUBJECT TERMS
Affordability, Ballistic Impact, Carbon/Epoxy, Damage Tolerance, Nondestructive Evaluation

16. SECURITY CLASSIFICATION OF:			17. LIMITATION OF ABSTRACT:	18. NUMBER OF PAGES	19a. NAME OF RESPONSIBLE PERSON (Monitor)
a. REPORT	b. ABSTRACT	c. THIS PAGE			Arnold Mayer
Unclassified	Unclassified	Unclassified	SAR	52	19b. TELEPHONE NUMBER *(Include Area Code)* (937) 255-5232

Standard Form 298 (Rev. 8-98)
Prescribed by ANSI Std. Z39-18

Table of Contents

Section **Page**

List of Figures…….iv

List of Tables……...v

1. Overview of the Project……...1
1.1 Background……..1
1.2 Summary of Accomplishments……2
1.2.1 Technical Tasks……...2
1.3 Personnel Involved……..3

2. Ballistic Impact Testing of Affordable Woven Carbon/Epoxy Composites……...4
2.1 Introduction……4
2.2 VARTM……..……7
2.3 High Velocity Impact Testing….……8
2.4 Ballistic Impact Study on Woven Carbon/Epoxy Composites with Polycarbonate Facing……...…8
2.4.1 Specimen Fabrication……..8
2.4.2 Results and Discussion…….....10
2.5 Ballistic Impact Studies on Stitched/Unstitched Woven Carbon/Epoxy Laminates……14
2.5.1 Specimen Fabrication……14
2.5.2 Ultrasonic NDE.……...……..15
2.5.3 Results and Discussion……..16
2.5.3.1 Unstitched Laminates……17
2.5.3.2 Stitched Laminates……20
2.6 Effect of Projectile Shape on the Ballistic Perforation of VARTM Carbon/Epoxy Composite Panels……25
2.6.1 Introduction……...25
2.6.2 Specimen Fabrication……27
2.6.3 Results and Discussion……..28
2.6.3.1 Impact Testing……...28
2.7 Analytical Modeling……..32
2.8 Summary……34
2.8.1 Studies on Plain and Twill Weave Samples with Polycarbonate Facing……...34
2.8.2 Studies on Stitched/Unstitched Plain and Satin Weave Laminates……...34
2.8.3 Influence of Projectile Shapes……...35

3. References……...36

4. Bibliography……...38

List of Acronyms……....41

List of Figures

Figure **Page**

1. Schematic of VARIM Process…….....7
2. Ballistic Impact Test Setup…….....8
3. a) Plain Weave Fabric, and b) 2/2 Twill Weave Fabric.……..……...9
4. Quantitative Measurements on Back Face a) Back View, and b) Side View..……10
5. Failure Mode Below Ballistic Limit a) all Plain, b) all Twill, c) Hybrid, Plain on Back, d) Hybrid, Twill on Back……11
6. Failure Mode at Ballistic Limit a) all Plain, b) all Twill, c) Hybrid, Plain on Back, d) Hybrid, Twill on Back…….....12
7. Undulations in a) Plain weave, b) 2/2 Twill Weave……12
8. Absorbed Energy Versus Ballistic Limit Velocity for Constituent and Hybrid Samples.……13
9. Melting of Polycarbonate Facing……..14
10. Stitching of Dry Fabric Preform, a) Stitching Operation b) 12.7 mm Stitched Preform...……...15
11. Front and Back Surfaces of 7-Layer Plain and Satin Weave laminates……17
12. Front and Back Surfaces of 17-Layer Plain and Satin Weave laminates……..17
13. Front and Back Surfaces of 37-Layer Plain and Satin Weave laminates……..18
14. Variation of Ballistic Limit with Number of Layers……18
15. Plain Weave Fabric a) Planform and b) Section……...19
16. Schematic of 8-Harness Satin Weave Fabric Laminates a) Planform and b) Section……...19
17. Ultrasonic C-Scan Images of Unstitched Impacted Plain and Satin Weave Laminates……21
18. Front and the back surface of 7-Layer Stitched Woven Carbon/Epoxy Samples Subjected to Ballistic Impact Loading with the Corresponding Ultrasonic C-Scan Images…….....23
19. Front and the Back Surface of 17-Layer Stitched Woven Carbon/Epoxy Samples Subjected to Ballistic Impact Loading with the Corresponding Ultrasonic C-Scan Images…….....24
20. Comparison of Ballistic Limit for Different Laminate Configurations (17 layers)……..25
21. Comparison of Ballistic Limits a) 12.7-mm Grid, b) 25.4-mm Grid……26
22. Projectile Shape and Dimensions..……27
23. Quantitative Measurements on Back Face……28
24. Energy Absorbed at Ballistic Limit Velocity for Each Specimen…….....29
25. Back Face damage of a) Fragment Simulating, b) Hemispherical, c) Conical, D) Flat Projectiles for 6.5-mm Thick Panels……....29
26. Average Transverse Crack Growth for Each Specimen……30
27. Back Face Damage of a) Fragment Simulating, b) Flat, c) Hemispherical, and d) Conical Projectiles for 3.2-mm Thick Panels ….……..31
28. Average Longitudinal Crack Growth for Each Specimen……31
29. Predicted and Experimental Ballistic Limit Velocity for the 6.5-mm Thick Panels……33
30. Predicted and Experimental Ballistic Limit Velocity for the 3.2-mm Thick Panels……34

List of Tables

Table **Page**

1. Specimen Nomenclature……..9
2. Details of Samples and Projectile……....9
3. Visible Percent Back Face Damage at V_{BL}……...……10
4. Ballistic Test Data……..14
5. Woven Carbon/SC-15 Epoxy Panels for Ballistic Impact Test…….15
6. Ballistic Test Results for 7-, 17-, and 37-layer Unstitched Woven Carbon/Epoxy Laminates…….16
7. Ballistic Test Results for 7, 17-layer Stitched Woven Carbon/Epoxy Laminates…….....22
8. Sample Number, Sample Thickness……..26
9. Sample Number, Velocity at Ballistic Limit, Energy Absorbed…….…..27
10. Sample Number, Average Transverse Crack Length, Average Longitudinal Crack Length……28

1. Overview of the Project

1.1 Background

Among several technologies identified in the Air Force Initiatives on Today's aircraft flying tomorrow (TAFT), Survivable Aircraft Structures and Affordability issues assume critical importance. Future aircraft technology enhancements (FATE) develop revolutionary technologies that will become the foundation for next-generation war fighters. Examples of FATE technologies include, among others, affordable LO data system; active aeroelastic wing; robust composite sandwich structures; damage tolerant/resistant composite structure; advanced composite inlets; photonic vehicle management systems; self-adaptive flight controls; and electric actuation.

The structures thrust of the Air Vehicles Directorate further supports the Air Force need toward a composite affordability initiative (CAI). Affordability and survivability are keys to air and space vehicles for higher performance, longer life and cost effectiveness. Newer structural concepts and design techniques need to be exploited for the latest materials, processes, and manufacturing technologies to produce more durable structures at lower weight and cost. The work carried out under this grant addressed several key issues pertaining to survivability of composite affordability in aircraft and space vehicles technologies, which make significant contributions toward Air Force needs. The vision was to enable future, affordable systems with increased performance, survivability, reliability and maintainability.

Conventional laminates are made with unidirectional prepregs using autoclave-molding process. Prepregs as well as autoclave molding method are expensive. However, with the advent of low-cost liquid molding processes the cost of production has been drastically reduced. Resin transfer molding (RTM) and vacuum assisted resin infusion molding (VARIM) process are two manufacturing approaches that hold promise for producing large-scale structures. As such, they are gaining acceptance for applications in armored vehicles, aerospace structures, naval/marine, and automotive applications. Both processes offer cost benefits over conventional autoclave molding through near net shape manufacturing and reduced number of parts. In the case of VARIM, low-pressure requirements translate into significantly lower tooling costs. In addition, woven fabrics, due to their ease of handling and greater drapability, have become excellent candidate reinforcement materials for VARIM processes. Due to the interlacing of fibers in two mutually perpendicular directions, woven fabric composites offer excellent resistance to impact damage. Normally, impact damage is initiated as matrix cracks, which extend to the interface of two laminae and progress as delamination. Matrix cracks initiate as either tensile or shear cracks. In both cases, the crack initiates transverse to the fibers within a ply. They propagate through the thickness when they come across stiffer fibers in the ply, leading to development of delamination. The extent of delamination will depend on the portion of impact energy available to fracture the interface. In the case of thin unidirectional laminates, the ply on the back surface splits open during the impact event, and the splitting leads to the large delamination. This process triggers generation and propagation of multiple delaminations, which leads to the reduction in residual properties, especially in compressive strength. In comparison, the plain weave fabric composites offer considerable advantage. In plain weave fabric composites, fibers run in both directions and are woven such that the fiber tows in each direction run above and below every alternate tow in the other direction. Assume that a crack is initiated within the ply. When it tries to propagate through the thickness, it will have to cut through the fiber in the fill direction. It will not be able to pass across the fiber in warp direction either. Hence, the delamination initiation and growth will be suppressed. This will help in considerably reducing the delamination damage. Hence, the residual compressive strength is not greatly reduced. In addition, stitching the dry fabric with high-strength Kevlar threads will further enhance the damage resistance.

It is seen from the open literature that information on the response of textile composites manufactured through such processes under impact loading was generally lacking. With the view of survivability and affordability in mind, the research addressed the key issues of affordable composites structures and their survivability to low-velocity, high-strain rate and ballistic impacts, their damage tolerance, and durability to long term fatigue. The specific research objectives were as follows:

1. To address the survivability aspects of the Air Force's CAI.
2. To manufacture conventional aerospace laminates and incorporate innovative concepts to produce damage-tolerant and functional designs using affordable low-cost processes for air and space vehicle structures.
3. To investigate survivability in terms of dynamic response to a variety of composite constructions in terms of low-velocity impact, high-strain rate impact, and ballistic impact scenarios.
4. To assess the survivability of affordable composite structures through post impact fatigue and residual strength studies.

1.2 Summary of Accomplishments

1.2.1 Technical Tasks

The technical tasks outlined above were accomplished by collaborative efforts between the prime contractors Tuskegee University (TU) and the sub contractors The University of Alabama in Birmingham (UAB), North Dakota State University (NDSU), North Carolina A & T University (NCA&T), and the University of Pittsburgh (UP) over a period of 3½ years.

Carbon/epoxy laminates were manufactured using affordable VARIM process using aerospace grade woven fabrics. Three weave architectures were considered in the study. They were plain, twill, and satin weaves. In most of the cases, the resin system used was SC-15 epoxy. The thickness of laminates manufactured ranged from 3 to 12 mm. Most of the fabrication was carried out at TU, NDSU, NCA&T and UAB. To enhance the damage resistance, through the thickness stitching was adopted. Three-cord Kevlar thread was used to stitch the laminates in orthogonal square grid fashion of size 12.7 mm and 25.4 mm.

Research work on the ballistic impact testing was carried out jointly by NDSU, TU, and UAB. Ballistic impact tests were carried out at NDSU and UAB. Impact damage was characterized through ultrasonic non destructive evaluation (NDE) at TU. Panels made of stitched/unstitched plain, satin, and twill weave of different thickness were characterized. In the second phase of the study, hybrid laminates made of different combinations of plain and twill weaves were studied. To improve the damage tolerance of the laminates, some of the panels were bonded with a tough polycarbonate layer and tested with the polycarbonate layer facing the impactor. The polycarbonate layer, being very tough, absorbs a large portion of impact energy, thereby protecting the backing structural composite laminate. To understand the effect of projectile shape, ballistic impact tests were carried out on 3.5- and 6.15-mm-thick laminates using four different shapes that included pointed tip, fragmented simulating projectile (FSP), and hemispherical and cylindrical ends. Ballistic limits were evaluated in all the tests. In all the laminates, the damage was localized and was dominated by penetration rather than delamination. This results in laminates with lower damage size with increased residual mechanical properties as compared to unidirectional laminates. Further, the damage modes were verified through ultrasonic NDE characterization. Detailed discussions on manufacturing and ballistic impact characterization are presented in this volume.

High strain rate impact tests were carried out at TU and UP. At TU, high strain rate compression tests were carried out on both stitched and unstitched laminate samples using a Split Hopkinson's Compression Pressure Bar setup. Both plain and satin weave samples were considered. Preliminary studies were carried out on unidirectional and cross-ply laminates. The response of woven fabric laminates was compared with that of unidirectional and cross-ply laminate samples. Off-axes tests were carried out to evaluate the performance of plain and satin weave samples. At UP, dynamic tests were carried out on conventional laminates made using prepregs as well as the woven fabric composite samples supplied by TU. High-speed photography was used to capture the dynamic deformation of the samples. Volume 2 presents the details of the high strain rate characterization.

Low-velocity impact characterization was carried out at TU and NCA&T. At TU, both stitched and unstitched laminates made of 7 and 17 layers of plain and satin weave carbon fabrics with SC-15 epoxy resin system at different energy levels. Impact damage was assessed by ultrasonic NDE technique. Again, the damage was confined to the location of impact and was dominated by indentation and penetration rather than delamination. Satin weave laminates offered better impact resistance as compared to plain weave laminates due to much straighter weave architecture. Further, stitching enhanced the damage resistance by confining the damage within the stitch grid. At NCA&T, parametric studies were carried out to study the effect of thickness on the impact response of the laminate. Laminates made of 8, 16, and 24 layers were considered. Post impact compressive strength was evaluated. Further, tests were carried out to evaluate post-impact fatigue performance. Volume 3 of the report provides the details of the low-velocity impact studies.

1.3 Personnel Involved

Tuskegee University

Faculty: Dr. Mahesh Hosur, Dr. Shaik Jeelani
Graduate Students: Mr. Madhu Adya, Mr. Jacob Alexander
Undergraduate Students: Mr. Marcus Hindmon, Ms. Davina Booker, Ms. Marquitta Johnson

North Dakota State University and The University of Alabama in Birmingham

Faculty: Dr. Uday Vaidya
Graduate Students: Biju Mattew, Ashwin Koleshwar (both NDSU), Shane Bartus, Chad Ulven (both UAB)
Undergraduate Students: Chad Ulven, Scott Nelson, Shane Bartus (NDSU)

North Carolina A & T University

Faculty: Dr. Ajit Kelkar
Graduate Students: Barry Blount (Graduated with MSME), Arlene Williams (Graduated with MSME), Ronnie Bolick (Pursuing PhD)
Undergraduate Students: Brandon Donnell, Ebonni J. Adams, Jermaine M. Bradley

The University of Pittsburgh

Faculty: Dr. Sylvanus Nwosu
Graduate Students: Ali Al-Quraishi, Femi Ojo

2. Ballistic Impact Testing of Affordable Woven Carbon/Epoxy Composites

Woven fabric composites are being increasingly used in composite structures for applications in the aircraft, marine, and automotive industries. With emerging low-cost processing techniques for composite materials, the role of fabric architectures in sustaining low- and high-velocity impact loads is a subject of interest. An example of a low-cost process is the out-of-autoclave, vacuum-assisted resin transfer molding (VARTM) technique. The present study evaluates the ballistic impact response of aerospace-grade structural woven carbon fabric laminates processed by VARTM. A series of ballistic impact tests were carried out on variety of laminate types which include unstitched plain weave, twill weave, and satin weave laminates of different thicknesses; hybridized laminates made of two different fabric weaves; stitched plain and satin weave laminates of made of 7 and 17 layers with two orthogonal grid sizes of 12.7 and 25.4 mm. Further, tests were carried out to determine the effect of different projectile shapes on the impact response of the laminates. In all of the tests, the laminates were made using the affordable VARTM process. Details of the tests and the results are discussed in this section.

2.1 Introduction

Fiber-reinforced polymer matrix composites have been widely used in aircraft, aerospace, marine, and automotive structures due to their high specific strength and stiffness [1]. One concern among polymeric composite designers is the response to low- and high-velocity impact loading. While several studies have addressed the low-velocity impact of composites [2, 3], studies on high-velocity impact are of equal interest [4-8]. Studies have addressed low- and high-velocity impact of composites with FSP [2-9].

Another issue that limits the usage of composite structures is cost. Currently, composite components in aerospace industry are mostly made of unidirectional laminates fabricated using prepregs. Prepregs are expensive materials and require stringent storage requirements and expensive manufacturing processes like autoclave molding. In addition, prepregs have limited shelf life. Also, any innovative concepts like through-the-thickness stitching is difficult to incorporate. While prepregs are very useful in forming simple folds and curves and to produce T-, L- and I-shaped components, they are not very attractive for complex curvatures. If complex structural components are to be made of unidirectional prepregs, they have to be produced from smaller, simple parts, which, increases the cost of assembly. Over 70 percent of the cost of composite structures is due to assembly and layup [10]. Further, cost of the prepreg scrap is about 40percent of the original material (less than 2/3 of the purchased prepreg ends up on the component). Hence, manufacturers and potential users of advanced composites are adopting alternative approaches. As such, liquid molding processes offer great potential for reducing layup and assembly costs. One such technique is VARIM [11, 12]. By using dry woven fabrics, it is possible to produce complex 3-D preforms due to greater drapability of the fabric. There is a direct route to manufacturing with fewer parts. Such integrated parts reduce the cost associated with tooling, layup operations, part counts and fasteners. The added advantages include increased dimensional tolerance, outlife of raw materials (fibers), reduced cycle times, near net molded components, reduced post molding process, and less material scrap.

With emerging low processing methods like VARTM, the process-performance relationships to various loading threats need attention. Further, high-velocity impacts with various geometries are of equal interest. The structures of interest in defense applications are commonly composed of woven fabric carbon/graphite, kevlar, and glass fiber-reinforced polymer matrix composites. Among these, carbon/graphite fiber composites are susceptible to impact damage due to their poor impact resistance, and are the focus of the present work. The use of woven fabrics in composite structures is continually

increasing. Woven composites possess high ratios of strain to failure in tension, compression, or impact loads due to the interlacing of the fiber bundles [13]. Several studies report the determination of in-plane properties of woven fabric composites [13-15].

Recent studies [16] have demonstrated utility of using a sacrificial tough polycarbonate layer bonded to carbon fiber composite to improve the impact resistance. Polycarbonate is a tough, dimensionally stable, transparent thermoplastic and is a suitable candidate material for many applications that demand high performance under repeated blow, shattering, and spalling [16]. It is characterized as the highest impact-resistant thermoplastic material within a temperature range of –40 °F to 280 °F. The use of polycarbonate as a facing for carbon/epoxy laminates is attractive, as the laminate can be designed for lower thickness, yet could sustain desired impact loading, thereby translating to cost savings.

One of the aims of present study is to investigate to what extent projectile geometry influences the damage propagation and evolution during ballistic impact normal to carbon/epoxy composite panels. Studies have addressed the effect and optimization of projectile shape during the ballistic impact of fiber reinforced plastic laminates [17-22]. The present work aims to investigate to what extent the crimp/undulation of woven fabric influences ballistic impact performance of the composite. A common consideration in this study is the presence of a sacrificial polycarbonate facing to the carbon/epoxy laminate. The facing shares a large portion of the initial impact load and damages upon impact. Previous studies have reported that in-plane properties of woven composites [2, 13-15] are reduced due to the crimp of the weave. The differences in the plain and 2/2 twill weave are relatively small in terms of crimp/undulation of the interlacing yarn when the loading direction is transverse to the yarn, such as an impact event. Experimental studies pertaining to the influence of high-velocity impact loading of plain and twill weave fabric composites bonded to a polycarbonate sheet are reported in this study. The influence of hybridizing the plain and twill woven fabric composites has also been considered. The rationale for hybridizing plies is twofold. Hybridization may be either the design intent to vary in-plane elastic properties, or a consequence of stacking variations that occur during processing, that may result in less than an ideal stacking condition, thereby resembling a hybridized weave.

Wen [17, 18] investigated the penetration and perforation of FRP laminates using flat-faced, hemispherical-ended, conical-tip and truncated-cone-nose projectiles in high-velocity impact. Using data collected from previous studies, Wen was able to develop analytical equations for predicting the penetration and perforation for each shape of projectile. These models are based on the assumptions that deformations during a ballistic event are localized and that the mean pressure from the laminate to resist the projectiles consists of both quasi-static resistive pressure due to elastic-plastic deformation, and dynamic resistive pressure due to velocity effects.

Ben-Dor et al. [19, 20] developed a model for determining penetration of monolithic semi-infinite and finite FRP laminates struck normally by arbitrary-shaped 3-D projectiles. Equations were derived to predict the penetration and perforation characteristics. A universal 3-D conical impactor was introduced as an optimal striker against the finite-thickness and semi-infinite shields. Problems arising from the design of an optimal projectile shape and analysis of the protective properties of composite materials were also discussed.

Gellert et al. [21] presented ballistic perforation data and post perforation microstructural measurements for flat, conical, and FSP's of different dimensions impacting glass-reinforced plastic (GRP) panels.

Energy to penetrate versus panel thickness was fitted to simple bi-linear plots. Analysis of the data explained that the indentation phase absorbs the most energy during a ballistic event and should be maximized in any bonded composite armor design. It was also shown that energy absorption in thin GRP panels is independent of projectile shape, and thin GRP and Kevlar targets respond similarly on a thickness basis against FSP's.

Lee and Sun [22] performed an experimental and numerical study concerning the dynamic penetration of clamped circular carbon fiber reinforced plastic (CFRP) laminates by flat-ended projectiles. The penetration process of composite laminates impacted by flat-ended projectiles was determined to be composed of three stages: pre-delamination, post-delamination before plugging, and post plugging. A computational model was established to explain the static punch process. The simulated punch curve was used in the subsequent dynamic impact analysis, and the displacements at certain specific checkpoints were adopted as the penetration criteria. This model was established to predict ballistic characteristics of graphite/epoxy laminates without performing dynamic penetration experiments.

In the current study, a series of ballistic impact tests were performed on eight-harness satin weave carbon/epoxy laminates of two thicknesses. Four different projectile geometries were used during high-velocity impact: hemispherical, conical, fragment simulating, and flat tip. The perforation mechanism, ballistic limit, and damage evolution of each laminate was analyzed. Wen's analytical models [17, 18] were used to predict ballistic limit of carbon/epoxy laminates.

When subjected to impact loading, inelastic energy in composites is absorbed in the form of creation of new surfaces. The failure mechanisms include matrix cracking, delamination, and ply splitting which taken together reduce the residual mechanical properties of the laminate considerably. Hence, in the past couple of decades, material science researchers have invested their efforts to address the delamination issues. Methods of reducing interply delamination include the use of tougher matrix systems, woven fabrics and through-thickness reinforcement. The main methods of through-thickness reinforcement include 3-D weaving, pinning, and stitching, of which stitching has been demonstrated to be most effective in improving the delamination resistance [23-35]. The early attempts of improving delamination resistance were made by Huang et al. [23] in the late 1970s, where steel wires of 0.33 mm diameter were placed at ±45° angles to the thickness of the laminate separated by 1.6mm. But embedding the steel wires by hand was not practical. In the mid 1980s Mignery et al. [24] explored the possibility of stitching fiber threads into the fabric preform before curing of the resin. As per Kang and Lee [25], the stitched composite laminate tolerates out-of-plane load and absorbs more energy during interlaminar crack growth, due to which the damage area is restricted and the integrity of the structure is preserved. Further, stitching appears to be the most cost-effective process for manufacture of damage-tolerant composite structures.

The following specific tasks were accomplished under ballistic impact studies of woven fabric composite laminates process by VARTM technique:

1. Ballistic impact testing of plain weave, twill weave, and hybrid of plain and twill weave laminates
2. Ballistic impact testing of laminates with polycarbonate facing
3. Ballistic impact characterization of plain and satin weave laminate with and without stitching
4. Effect of projectile shape on the impact response of satin weave laminates

Following sections will discuss the details of manufacturing of laminates, the ballistic impact test setup and results of each of these tasks.

2.2 VARTM

In all these tasks, laminates were manufactured by VARTM process. For fabricating the laminate, freekote (mold-releasing agent) was sprayed on the mold. The required number of layers was carefully placed on the mold. Then a sealant tape was tacked on the surface of the mold about 25 to 50 mm from the perimeter of the fabric layers. Resin supply tubes were connected to the system with the mold end of the tube connected to a spiral wrap along with a distribution mesh that lies on top of the preform. This facilitates easy flow of resin over the top and through the thickness of the laminate when vacuum is applied. Tubes linking the vacuum pump and the spiral wrap were also connected. Resin traps were placed between the vacuum pump and the mold to collect the excess resin. Finally, a vacuum bag was placed on the mold and pressed firmly against the sealant tape to provide a vacuum tight system. The preform was left to debulk under vacuum. After debulking, the SC-15 resin system was infused, impregnating the fabric as the resin flow advanced toward the vacuum side. The resin inlet valve was closed when resin reached the suction side, and the infused laminate was left to cure at room temperature. Vacuum pressure was maintained until the end of the cure to remove any volatiles generated during the polymerization, in addition to maintaining the pressure of one atmosphere. Arrangement of the fabrication process is detailed schematically in Figure 1.

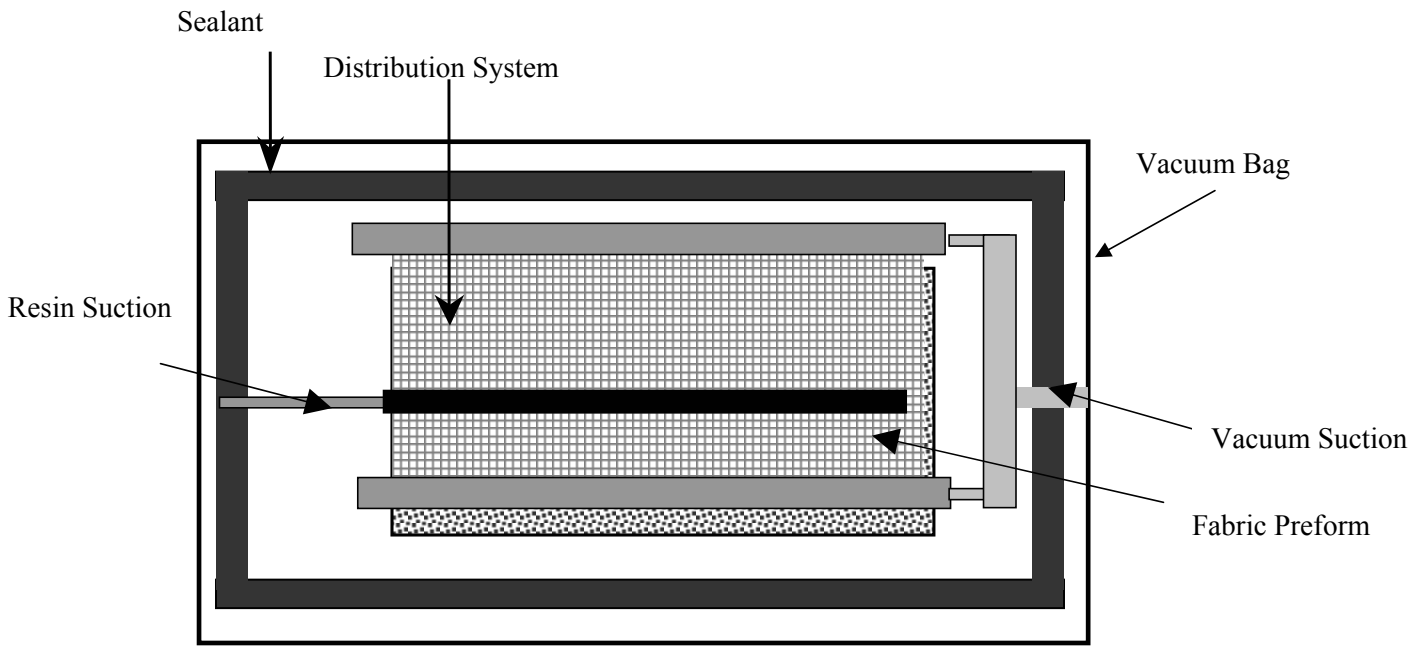

Figure 1. Schematic of VARIM Process

2.3 High Velocity Impact Testing

The high-velocity impact tests were performed using a gas-gun test set up (Figure 2). Foam sabot carriers (8 g) with FSP (14 g) were used. The gun consists of a 3-m barrel, a firing chamber, and a capture chamber. The sample is placed in the capture chamber. Sabo-assisted projectiles can be launched to velocities of 200 m/sec. A sabot stripper plate mounted in front of the muzzle was used to separate the projectile from the launching sabot before impacting the target. Samples of dimension 125 by 125 mm (5 by 5 inches) were used. The sample was mounted in a simply supported boundary condition along its four edges sandwiched on rollers between two rigid aluminum plates. Two chronographs (Model-Prochrono Digital) were mounted with clamps to the bottom of the capture chamber with a transparent optical window to record the incident and residual velocity of the projectile. Varying the pressure of gas in the firing chamber varied the impact velocity.

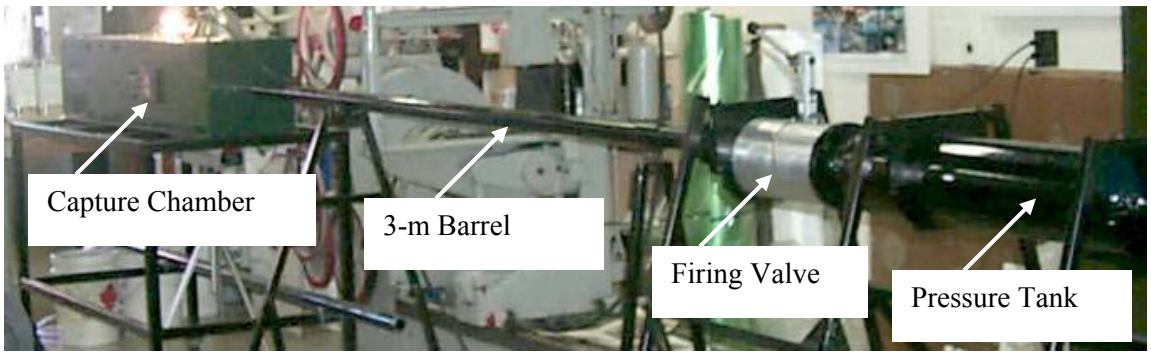

Figure 2. Ballistic Impact Test Setup

2.4 Ballistic Impact Study on Woven Carbon/Epoxy Composites with Polycarbonate Facing

This section describes the details of the experimental study carried out on plain and twill weave fabric composites under ballistic impact loading. The tests were carried out on plain and twill weave laminates as well as the hybrid laminates made of different combinations of plain and twill weave layers. Further, the tests were carried out on laminates with polycarbonate facing, which acts as a sacrificial layer facing the projectile.

2.4.1 Specimen Fabrication

For this study, composite panels were fabricated using plain (3K yarn, 12.5 by 12.5 count, 5.7 oz/sq yd, 0.2286 mm, tensile strength 1.17 GPa, 230 GPa, Figure 3a) and 2/2 twill (3K yarn, 12.5 by 12.5 count, 194.88 g/m^2, 0.3175 mm, Figure 3b) weave T300B-40B-3K-Toray carbon fabric and Applied Poleramic SC-14 epoxy resin through a VARIM process. The gel time of the resin was approximately three hours and the curing was completed in twelve hours. Three types of panels were fabricated, each containing seven layers of carbon fabric. They included a) all seven plain weave plies, b) all seven twill weave plies, and c) hybrid lay-up with four twill and three plain weave plies. The nomenclature for the panels is provided in Table 1. Each of these panels was bonded to a polycarbonate sheet (Clear PC (Lexan®), supplier-Precision Plastic and Punch Co.) of 2.5 mm thickness. The polycarbonate sheet was bonded to the composite on one side using 3M spray adhesive (Super 77). The average thickness of the plain weave laminate was 1.6 mm for twill and 1.7 mm for hybrid weave. The total thickness of the laminate and polycarbonate was 4.1 mm for the plain weave-polycarbonate, and 4.2 mm for the twill and hybrid weave-polycarbonate.

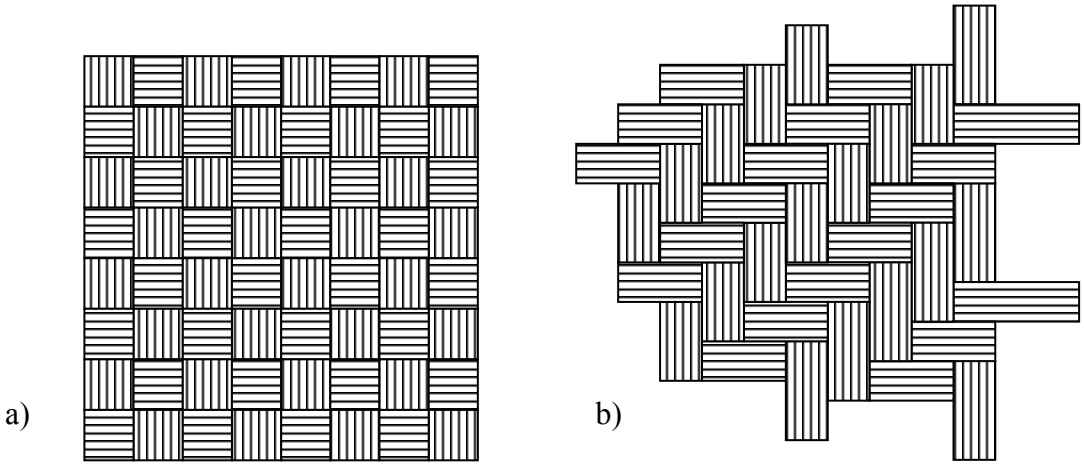

Figure 3. a) Plain Weave Fabric and b) 2/2 Twill Weave Fabric

Tests were conducted on four types of sample configurations: a) all plain weave, b) all twill weave, c) hybrid plain-twill weave with plain weave toward the back face, and d) hybrid plain-twill weave with twill weave toward the back face. In all tests, the polycarbonate sheet faced the impact side. At least three samples were tested in each category to ensure repeatability. Table 2 provides information on the projectile, the mass of the constituent laminate, and that of polycarbonate.

The impact tests were designed to investigate the damage evolution below, at, and beyond the ballistic limit. The ballistic limit velocity denoted by V_{BL} is considered the velocity at which the energy absorption was maximized. At V_{BL}, the projectile remains embedded in the panel, and in some instances penetrates fully. The projected damage in the sample was maximum at this condition. For tests 'below' the ballistic limit, the projectile rebounded from the panel and was recovered from the impact end. For beyond ballistic limit tests, the damage zone was smaller and penetration was complete. For the test velocities adopted here, the residual velocity was appreciable only for a few cases, as reported in Table 3.

Table 1. Specimen Nomenclature

PW7:	Plain weave, 7 layers
TW7:	Twill weave, 7 layers
PWT7A:	Plain & twill weave hybrid, 7 layers, plain weave on back
PWT7B:	Plain & twill weave hybrid, 7 layers, twill weave on back

Table 2. Details of Samples and Projectile

Polycarbonate sheet: average mass 43 g, volume 38.5 cm^3
Carbon laminate: average mass 35 g, volume 25.6 cm^3
Total mass of polycarbonate bonded to carbon plies: 78 g
Mass of FSP: 16 g, 12.7 mm diameter

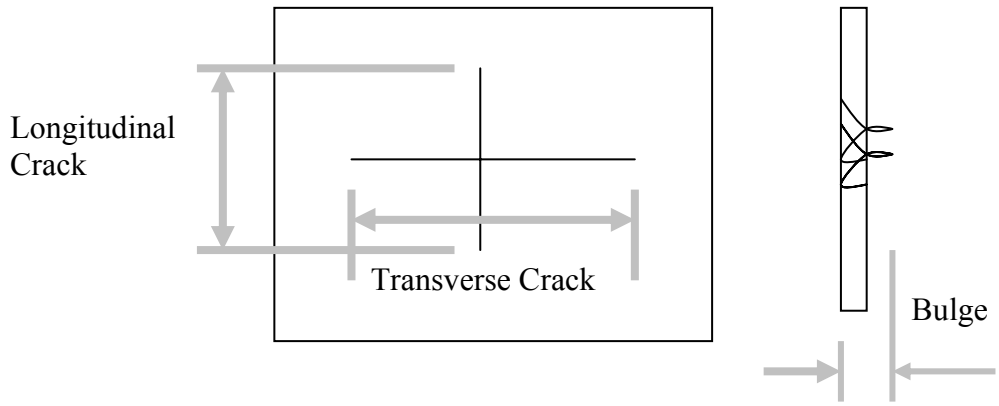

Figure 4. Quantitative Measurements on Back Face; a) Back View and b) Side View

2.4.2 Results and Discussion

The samples exhibited transverse and longitudinal cracking patterns, and these features were quantified. Besides measuring the incident velocity, the damage evaluation and assessment of failure modes of the target was carried out by measuring the parameters illustrated in Figure 4 with respect to the back face. These included - transverse crack, longitudinal crack, and back face bulge. These measurements provided information about the principle dimensions of the impact damage zone such as entrance and exit areas for perforation and the damage profile (shape, size, and location). Table 3 summarizes the damage observations and results for V_{BL}.

Table 3. Visible Percent Back Face Damage* at V_{BL}

Specimen	Transverse (percent)	Longitudinal (percent)	Bulge (percent)	V_{BL} (m/s)
PW7	28.4	22.5	168.3	100
TW7	26.5	24	54.8	120
PWT7-A	27.9	15.7	114.3	98
PWT7-B	29.4	26.5	54	105

*based on 101.6 mm by 101.6 mm (4 by 4 inches) simply supported sample

As reported in Table 3, the extent of transverse cracking of the back face was within 10 percent for the PW7, TW7 and PWT7-A and PWT7-B. However, the extent of longitudinal cracking is approximately 68percent higher for the PWT7-B samples as compared to the PWT7-A. Also, the TW7 exhibited 6percent higher longitudinal cracking than the PW7 samples. In all cases, the PW7 and PWT7-A samples exhibited a significant bulge on the back face due to formation of fiber shear zone. The bulge was measured to be 168 percent for the PW7 samples (211percent larger than the TW7), 114percent for the PWT7-A samples (111percent larger than the PWT7-B), and only 54percent for both TW7 and PWT7-B samples.

The energy absorption mechanisms in the plain weave dominant laminates was observed to be due to fiber shearing, therefore higher bulging and reduced longitudinal cracking were observed. In comparison, the twill-weave dominant laminates exhibited higher back (tensile) side cracking and less fiber shearing, which explains the small bulging of the back face.

Figure 5a-d represent the failure modes for the PW7, TW7, PWT7-A and PWT7-B laminates for the just below the impact limit condition. Below ballistic limit, the damage incurred by the twill weave laminates is smaller than the plain weave (Figure 5a versus 5b). The hybrid laminates appear to exhibit similar damage states. Figure 6a-d illustrates the same category of samples at ballistic limit. At the ballistic limit, the longitudinal cracking of the twill weave laminates is seen to be higher than for the plain weave. This is attributed to fiber shearing in the plain weave laminates. For the 2/2 twill weave, the undulations run over two tows and this small variation (of straightness of the 2/2 twill weave yarns) is seen to transition the failure mode to a tensile fiber fracture mode (with less shear bulging). Figure 7 a and b compare an idealized stacking of the plain and twill weave. The alternating over-under undulations of the plain weave (PW7) results in 20 percent lower ballistic limit than the twill weave (TW7) laminates. For the hybrid weave samples, the ballistic limit was 7 percent higher for the PWT7-B than the PWT7-A laminates, i.e., when the twill weave was on the back (tensile) side. Figure 8 demonstrates the bounds of energy absorbed versus velocity at ballistic limit for the different sample types. The hybrid samples, as expected, exhibit a ballistic limit characteristic in between that of the all-plain and twill weave. The lowest value of ballistic limit was obtained from the PWT7-A panels. This was perhaps because of the limited role of the twill weave layers, which were closer to the compression zone (impact side), and lesser plain weave plies subjected to shear during the passing of the projectile through the back side layers. This is also noted by the comparison of PW7 to PWT7-A. In comparison to the PW7, the shear bulge is lower for the hybrid PWT7-A laminate.

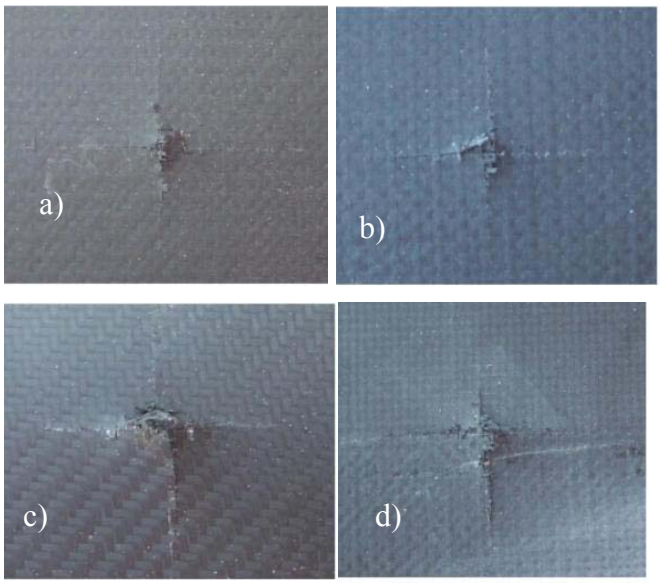

Figure 5. Failure Mode Below Ballistic Limit;
a) all Plain, b) all Twill, c) Hybrid, Plain on
Back, d) Hybrid, Twill on Back

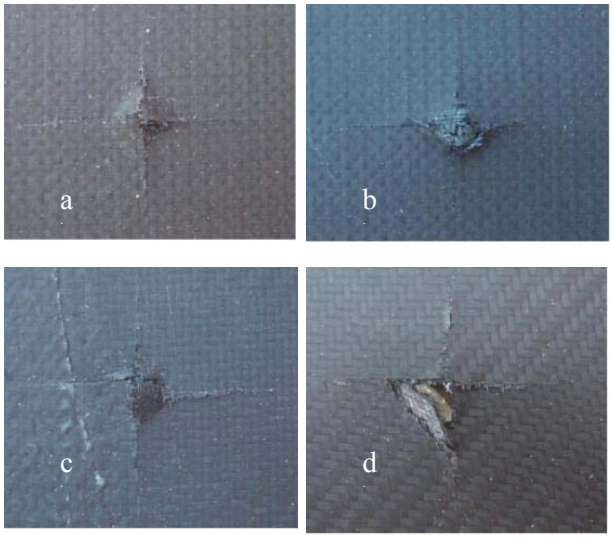

Figure 6. Failure Mode at Ballistic Limit; a) all Plain, b) all Twill, c) Hybrid, Plain on Back, and d) Hybrid, Twill on Back

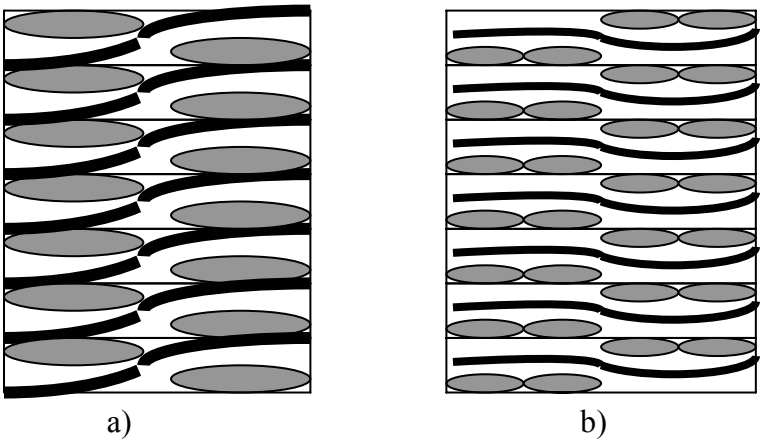

Figure 7. Undulations in a) Plain Weave, and b) 2/2 Twill Weave

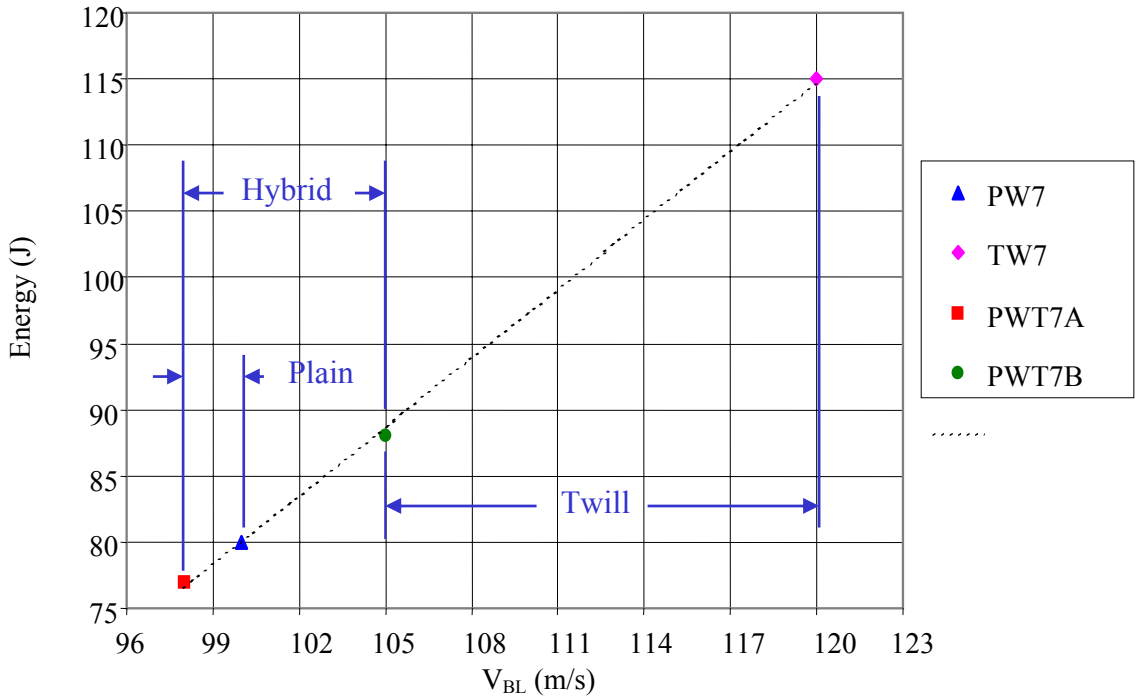

Figure 8. Absorbed Energy Versus Ballistic Limit Velocity For Constituent and Hybrid Samples

Table 4 summarizes the ballistic test data. For samples that exhibited perforation, only for the PWT73A sample was residual velocity recorded. For all other samples, the residual velocity was not appreciable enough to give an exit velocity reading. The projectile was recovered at the backside of the panel, indicating it had slowed down sufficiently to drop off after penetration. The incident energy for the samples is reported in Table 4 as well. For the ballistic limit velocities, this may be treated as the absorbed energy in the sample, neglecting energy loss at the supports. The TW7 sample exhibited the highest energy absorption (115 J), in comparison to 80 J for the PW7 samples. Hybridization did not provide significant benefits in terms of energy absorbed. The PWT7-B sample exhibited higher energy than the corresponding PWT7-A sample.

For all of the samples, the polycarbonate-facing exhibited localized melting at point of impact as shown in Figure 9, and a damage zone equivalent to the diameter of the projectile. The thickness of the polycarbonate was not sufficient enough to cause radial cracking within it. The role of the polycarbonate in all of the tests was to reduce the velocity of the projectile due to the mechanism of localized melting.

2.5 Ballistic Impact Studies on Stitched/Unstitched Woven Carbon/Epoxy Laminates

2.5.1 Specimen Fabrication

For this study, two fabric architectures were considered: plain and satin. Plain weave carbon fabric was of style 4060-6 with 10 oz/sq yard, and satin weave was eight-harness carbon fabric of style 5999 with 10.8 oz/sq yard supplied by Fiber Materials Inc. For unstitched laminates, 7, 17, and 37 layers of fabric were used. For the fabrication of stitched laminates, 7 and 17 layers of dry fabric were stacked together and stitched using 3-cord high-strength Kevlar thread with a pitch of 6 mm, with stitches forming a grid of 25.4 and 12.7 mm, respectively (Figure 10). All of the laminates were fabricated using VARIM. Specimens of nominal size 125 by 125 mm are cut from the laminates for testing. All of the samples were subjected to ultrasonic NDE to evaluate the extent of damage. Table 5 provides information on the samples tested in the current study.

Table 4. Ballistic Test Data

Sample	Vin (m/s)	Vout (m/s)	Energy (J)
PW71	85	0	58
PW74	89	0	63
PW72	**100**	0	80
PW73	122	-	119
TW71	109	0	95
TW74	**120**	0	115
TW72	131	-	137
PWT71A	88	0	62
PWT77A	**98**	0	77
PWT78A	102	-	83
PWT73A	128	63	131
PWT76B	82	0	54
PWT72B	83	0	55
PWT75B	**105**	0	88
PWT74B	127	-	129

Note: - Bold values represent at ballistic limit
-No values on V_{out} represent penetration, but no sufficient residual velocity to obtain a reading on the exit side

Figure 9. Melting of Polycarbonate Facing

a)

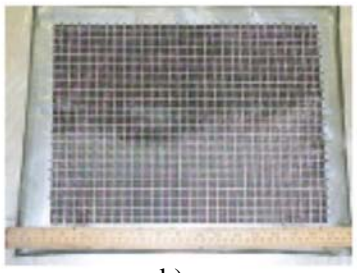

b)

Figure 10. Stitching of Dry Fabric Preform; a) Stitching Operation, and b) 12.7 mm Stitched Preform

Table 5. Woven Carbon/SC-15 Epoxy Panels for Ballistic Impact Test

Number of Layers	Thickness (mm), Plain weave	Thickness (mm), Satin weave
7	2.8	3.5
17	5.7	8.0
37	13.8	14.3

2.5.2 Ultrasonic NDE

Ultrasonic inspection of the laminates was carried out using a Krautkramer ultrasonic pulser receiver unit with TestTech mechanical system. The scanning was done in pulse-echo immersion mode using a 5-MHz 25.4-mm point focus sensor. In ultrasonic inspection, using the pulse-echo immersion mode, the sample was placed in a water tank and the transducer was brought over the sample. As the ultrasound propagates through the water medium, part of it gets reflected back from the top surface of the sample, which is called as the front surface echo, while the rest of it passes through the material. The part of the ultrasound that is propagating through the sample gets reflected back at the other end of the sample, which is called as back surface echo. If there is any defect in the path of the travel of ultrasound, then it acts as a reflector and a defect echo is obtained. Therefore, by collecting the information from the back surface echo of the ultrasound from the entire surface area of the sample, we can obtain the mapping of the defect in the sample, which is referred to as a C-scan. This is done by setting an electronic gate on the back surface echo and digitizing the signal. The digitized data is further analyzed by pseudo coloring to get a colored map to differentiate a defective area from the good area. Such scanning will give the information of cumulative damage as projected onto a horizontal plane.

In the current study, ultrasonic scanning was done with the impacted surface facing the sensor to get the information about the state of damage. The gate was set on the back surface echo. All of the laminates were subjected to ultrasonic NDE both before and after impact testing. The ultrasonic testing before impact loading was carried out to ensure that there were no fabrication defects in the sample. Post-impact ultrasonic testing was conducted to evaluate the extent of damage in the sample.

2.5.3 Results and Discussion

Ballistic impact tests were carried out on 7, 17, and 37 layered unstitched and 7 and 17 layered stitched laminates made using plain and satin weave fabric with SC-15 epoxy resin system. Samples were impacted using foam, sabot-assisted FSP weighing 14 g. Four samples were tested for each thickness to determine the ballistic limits. Results of the ballistic tests are shown in Tables 6 and 7. The impact tests were designed to investigate the damage evolution below, at, and beyond the ballistic limit. The ballistic limit velocity denoted by V_{BL} is considered as the velocity at which the energy absorption was maximized. At V_{BL}, the projectile remains embedded in the panel, and in some instances penetrates fully. The projected damage in the sample was maximum at this condition. For tests below the ballistic limit, the projectile rebounded from the panel and was recovered from the impact end. For beyond ballistic limit tests, the damage zone was smaller and penetration was complete.

Table 6. Ballistic Test Results for 7-, 17-, and 37-layer Unstitched Woven Carbon/Epoxy Laminates

Sample	Panel ID	Input Velocity (m/s)	Exit Velocity m/s)	Energy Absorbed (J)	Comments
Satin, 7 layers	5A	114	275	87	Over the ballistic limit
	5B	**86**	**0**		Just over the ballistic limit
	5C	46	0		Under ballistic limit
	5D	52	0.00		Under ballistic limit
Plain, 7 layers	6A	56	0		Under ballistic limit
	6B	**61**	**11**	**25**	Just over the ballistic limit, low exit velocity
	6C	75	13	38	Over the ballistic limit
	6D	71	33	28	Over the ballistic limit
Plain, 17 layers	7A	104	100	6	Over the ballistic limit
	7B	**102**	**12**	**72**	Just over the ballistic limit, small exit velocity
	7C	85	0.00		Under ballistic limit
	7D	error	68		Chronograph error in recording of the input velocity
Satin, 17 layers	**8A**	**171**	**0.00**		Just over the ballistic limit, small exit velocity
	8B	175	39	204	Over the ballistic limit
	8C	90	0		Under ballistic limit
	8D	100	0		Under ballistic limit
Plain, 37 layers	9A	111	0		Under ballistic limit
	9B	**232**	**0**		Ballistic limit, projectile was imbedded in the sample
	9C	265	48	474	Over the ballistic limit
	9D	error	0		Chronograph error in recording of the input velocity
Satin, 37 layers	10A	179	0		Under ballistic limit
	10B	**262**	**0**		Ballistic limit, projectile was imbedded in the sample
	10C	275	85	480	Over the ballistic limit
	10D	error	error		Chronograph error in recording of the velocity

Close to ballistic limit (boldfaced)
Exit velocities less than 6 m/s cannot be recorded by the chronograph

2.5.3.1 Unstitched Laminates

Figures 11-13 illustrate the front and back surfaces of the plain and satin weave samples impacted at or near the ballistic limit for 7, 17, and 37 layers respectively. The ballistic limit for plain and satin weave laminates is plotted as a function of the number of layers as shown in Figure 14.

Front Surface Back Surface

Plain Weave (61 m/s)

Front Surface Back Surface

Satin Weave (86 m/s)

Figure 11. Front and Back Surfaces of 7-Layer Plain and Satin Weave Laminates

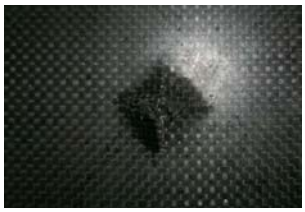

Front Surface Back Surface

Plain Weave (102 m/s)

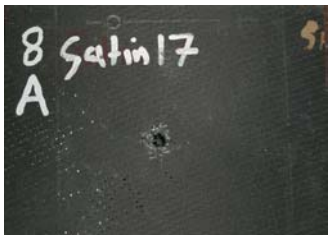

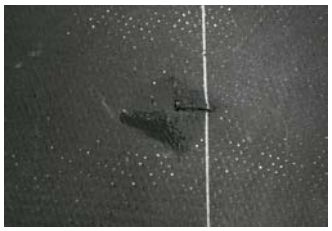

Front Surface Back Surface

Satin Weave (171 m/s)

Figure 12. Front and Back Surfaces of 17-Layer Plain and Satin Weave Laminates

Front Surface Back Surface

Plain Weave (232 m/s)

Front Surface Back Surface

Satin Weave (262 m/s)

Figure 13. Front and Back Surfaces of 37-Layer Plain and Satin Weave Laminates

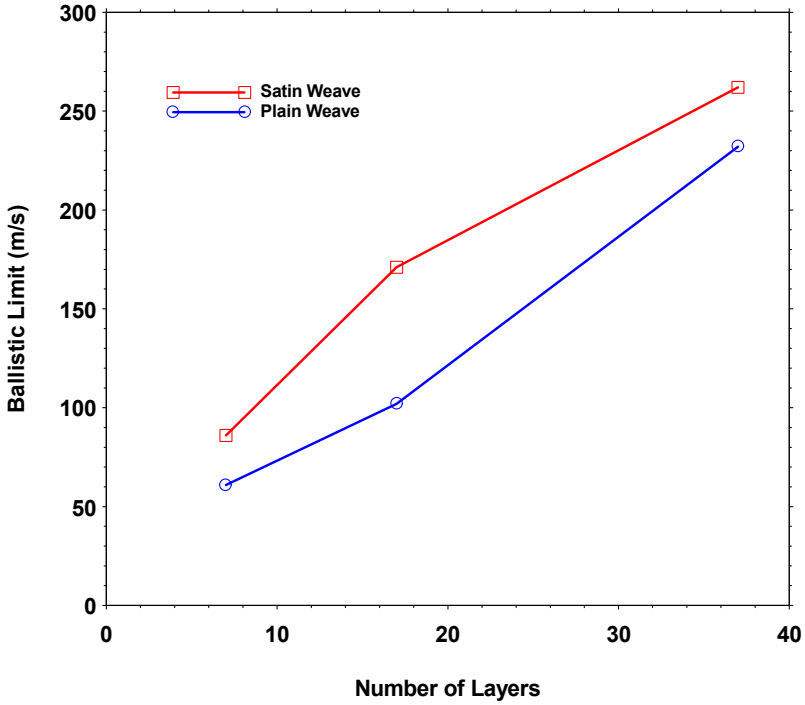

Figure 14. Variation of Ballistic Limit with Number of Layers

From Figure 14, it can be seen that the ballistic limit for satin weave laminates is much higher that the corresponding plain weave laminates. This can be attributed to two reasons. One, satin weave laminates are slightly thicker than plain weave laminates. Two, the fabric architecture. In the plain weave fabric, the fiber tow in the warp direction crosses over every other fiber tow in the fill direction, as shown in the schematic diagram in Figure 15. The angle made over the crossing, which is called crimp angle, is thus steep and is repeated for each tow in both fill and warp direction. Hence, there is considerable reduction in the in-plane properties of the laminate made using plain weave architecture. In comparison, in eight-harness satin weave fabric, the fiber tow in the warp direction runs over seven fiber tows in the fill direction before crossing under the eighth tow in the fill direction, as shown schematically in Figure 16. This pattern in repeated over the entire width of the fabric. This will result in much straighter architecture without any apparent indication of the weave. The resulting laminate will be very close to unidirectional laminate, with much higher in-plane properties as compared to plain weave fabrics. Under impact loading, the tensile failure initiates through in-plane failure of the bottommost ply. The fabric with better

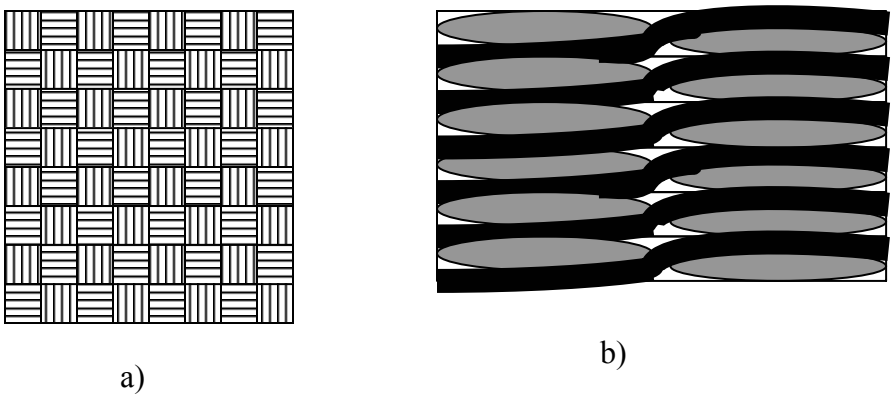

Figure 15. Plain Weave Fabric; a) Planform and b) Section

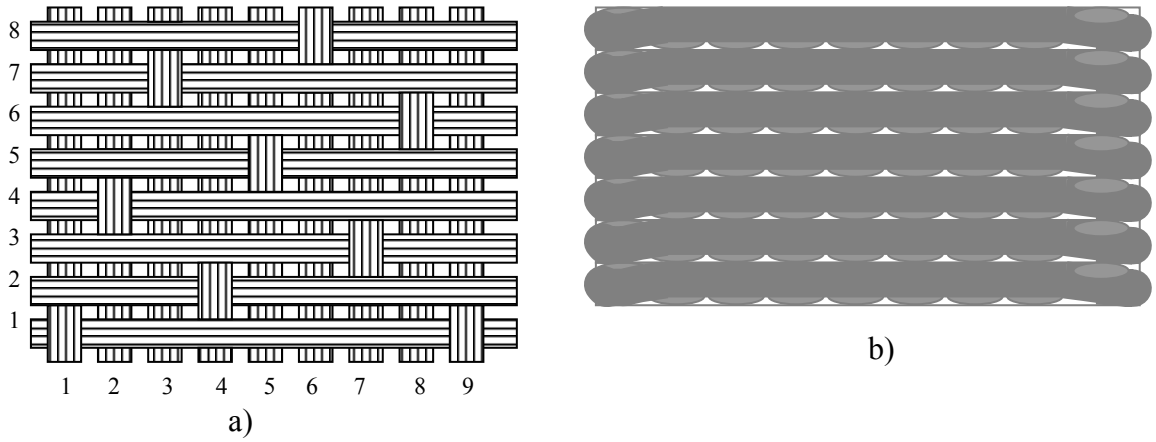

Figure 16. Schematic of 8-Harness Satin Weave Fabric Laminates; a) Planform and b) Section

in-plane properties would naturally sustain higher stresses, which in the current case is satin weave. Further, the failure initiation is more likely though tensile failure of the fiber tows. In the case of plain weave fabric, the failure initiation is more likely to be through shear fracture of the fiber tow.

The ensuing damage modes were evaluated through ultrasonic NDE. When the impact velocity is just below the ballistic limit, the projectile penetrates the laminate partially. All of the impact energy is then absorbed by the laminate. The modes of damage include removal of material by penetration, and multiple delaminations at the back surface with the maximum delamination being at the interface, where the projectile comes to rest. When the striking velocity is just above the ballistic limit, the laminates get penetrated completely, with lesser delamination damage. The damage size is smaller on the impact surface and more on the back surface. Again, the damage mode on the back surface is controlled by the weave architecture. Plain weave, being more closely knit, offers higher through thickness shear resistance than the satin weave laminate. This is quite evident if we look into the back surface more closely. Most of the plain weave samples show bulging or clear hole on the back surface, whereas the satin weave laminate exhibit tensile flexural failure as additional failure mode. Figures 17 a-f illustrates ultrasonic NDE images of the samples that were impacted with velocity to the ballistic limit for 7-, 17- and 37-layer laminates respectively. All the samples were scanned with both front and back surfaces facing the transducer. All of the 7- and 17-layered panels indicated damage by penetration, with very little delamination damage. The damage was restricted to the region close to the hole left by the bullet upon penetration. For the thicker 37-layer sample, all of the plain weave laminates exhibited through penetration damage as can been seen from the c-scan (Figure 17e). However, the 37-layer satin weave sample had partial penetration. This resulted in the creation of large delamination at the interface where the projectile was arrested (see Figure 17f). From these figures, it is quite clear that the damage modes are quite different for the two fabric architecture. Since the laminates were all of the same size, thicker laminate, being stiff, undergo relatively lesser deflection. Hence, the size of damage will be more as the thickness increases. Comparing the satin and plain weave laminates, it can be seen from the above figures that satin weave laminate suffers greater damage.

2.5.3.2 Stitched Laminates

It is know that, through the thickness stitching enhances the damage resistance of carbon/epoxy composites. In order to determine the influence of stitching on the response of the laminates to impact loading, 7 and 17 layer panels were fabricated with both plain and satin weave fabric. Through the thickness stitching was done using a 3-cord Kevlar thread using a stitching machine. The dry fabric layers were stacked together and stitched through the thickness. Orthogonal grids of size 12.7 mm and 25.4 mm were employed. The pitch of stitching along the stitch line was maintained at 6 mm. 8 sets of samples were subjected to projectile impact loading. For each set four samples were used to determine the ballistic limit. Table 7 lists the details of impact test results. Boldfaced numbers indicate the ballistic limit for each set of sample.

Figures 18 and 19 represent the front and back surfaces of 7-layer and 17-layered stitched plain and satin weave samples along with the C-scan images for both 12.7-mm and 25.4-mm stitch grids for the samples that were impacted close at their ballistic limits. In can be seen from the pictures of the back surfaces of both plain and satin weave samples and their C-scans that the splitting damage, which was seen in unstitched laminates, is missing. Though the woven fabric composites arrest the spread of backface damage by splitting due to the inherent interlacing nature of the fabric, at high impact energy, the back face fiber tows fail in tension and split, as we can see in the case of unstitched samples. However, in case of stitched samples, the splitting damage that is initiated due to the tensile failure of the backface gets

arrested at the location of the stitch line, as can be seen from the C-scans in Figures 18 and 19. Hence, the impact energy has to find alternate routes to transfer the energy. This is facilitated by spending the energy in penetration. During penetration, the projectile has to transfer its kinetic energy in shearing through the layers through the thickness of the laminate. The damage, which is already localized in the case of woven fabrics, gets further localized due to the constraints imposed by the stitch lines. Further, if the projectile impacts the laminate on the stitch line itself, then the laminate will split at the stitch line. Sometimes, the energy is expended in snapping the stitch lines. When the dry fabrics are stitched, the needle damages the fibers locally. Further, the region where the threadline holds the fabric through the thickness has localized resin-rich pockets. When the projectile impacts the sample at the stitch line, the fabric is sheared more easily in comparison with the fabric elsewhere.

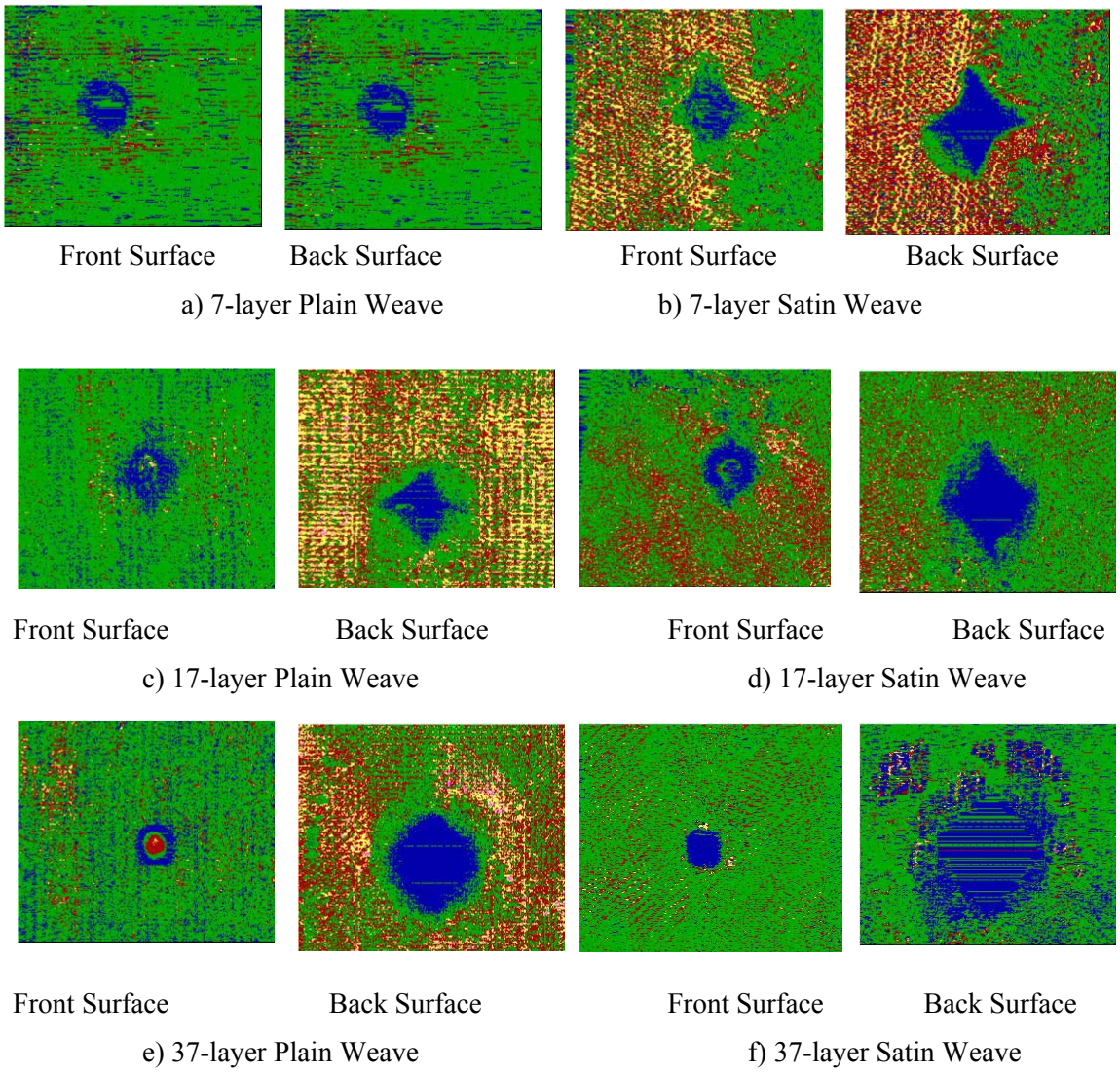

Figure 17. Ultrasonic C-Scan Images Of Unstitched Impacted Plain and Satin Weave Laminates

Table 7. Ballistic Test Results for 7-, and 17-layer Stitched Woven Carbon/Epoxy Laminates

Sample	Panel ID	Input Velocity (m/s)	Exit Velocity (m/s)	Energy Absorbed (J)
Plain weave 17 layers, 12.7- mm grid	1A	80	0	
	1B	**97**	0	66
	1C	error	0	
	1D	132	120	1
Satin weave 17 layers, 12.7- mm grid	2A	129	error	
	2B	**113**	**0**	**89**
	2C	98	0	
	2D	152	error	
Satin weave 7 layers, 25.4- mm grid	3A	53	<10	13
	3B	41	0	
	3C	59	30	6
	3D	**43**	**0**	**13**
Plain weave 7 layers, 25.4- mm grid	4A	39	0	
	4B	52	<10	13
	4C	49	0	
	4D	**50**	**0**	**18**
Plain weave 17 layers, 25.4- mm grid	5A	97	Error	
	5B	79	0	
	5C	92	0	
	5D	**88**	**0**	**54**
Satin weave 17 layers, 25.4- mm grid	6A	90	0	
	6B	97	52	14
	6C	92	0	
	6D	**94**	**0**	**62**
Satin weave 7 layers, 12.7- mm grid	7A	68	14	20
	7B	49	0	
	7C	**66**	**0**	**30**
	7D	73	error	
Plain weave 7 layers, 12.7- mm grid	8A	52	error	
	8B	47	0	
	8C	68	13	21
	8D	**61**	**<10**	**26**

Close to ballistic limit (boldfaced)
Exit velocities less than 20 ft/s cannot be recorded by the chronograph

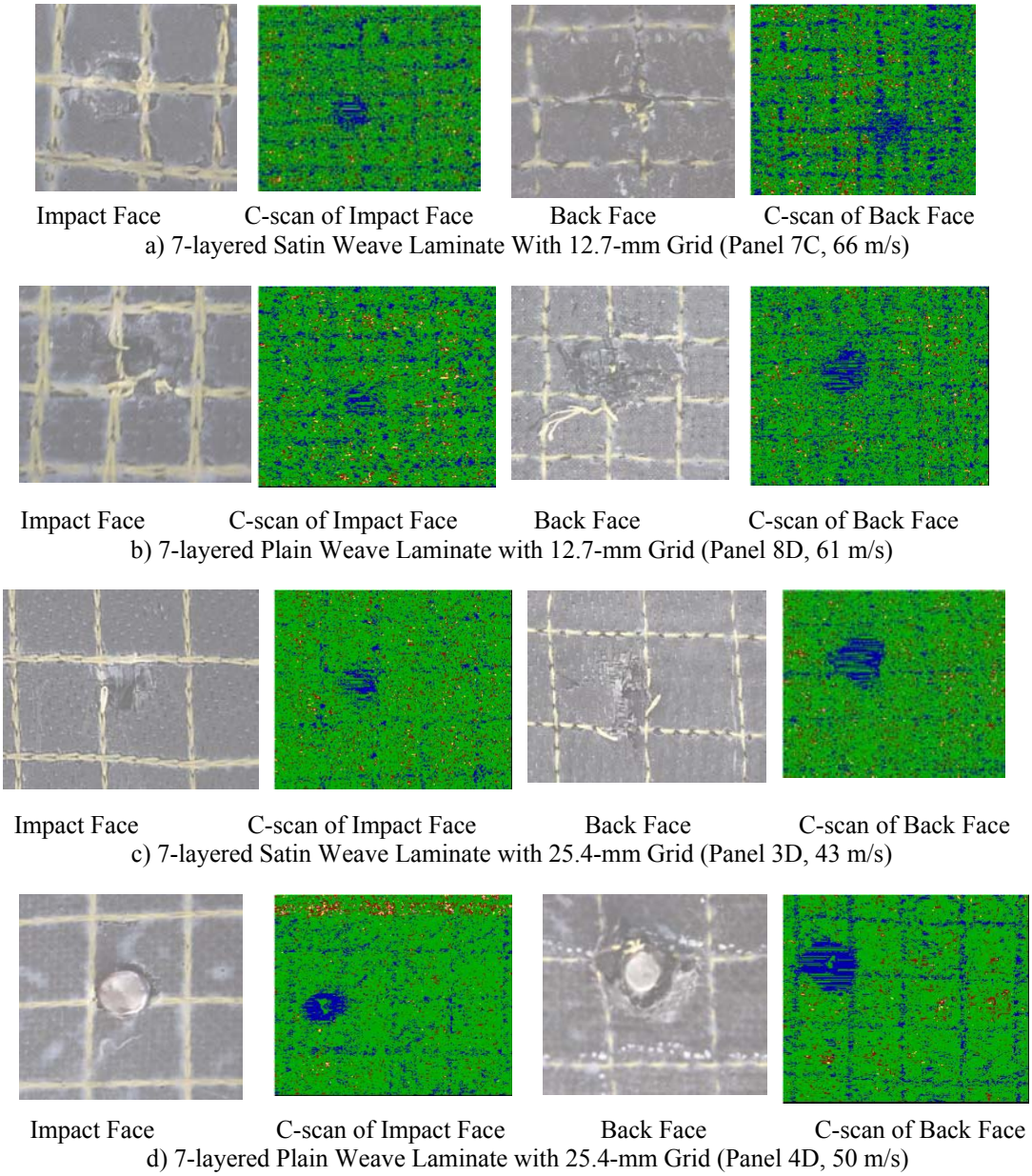

Figure 18. Front and the Back Surface of 7-Layer Stitched Woven Carbon/Epoxy Samples Subjected to Ballistic Impact Loading with the Corresponding Ultrasonic C-Scan Images

The damage size is lower in the stitched samples as compared to the unstitched samples. This will be highly desirable from the point of view of residual properties. The lower the damage size, the lower the reduction in the residual properties, which is desirable from the damage tolerance point of view. However, this leads to lowering of the ballistic limit also. The projectile will penetrate the stitched laminates at much lower incident velocities in compared to unstitched laminate. This will reduce the ballistic limit for stitched laminates (see Figure 20). Hence, the choice of opting for stitching of the

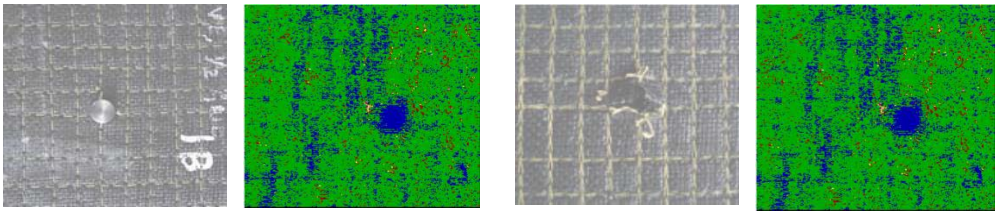

Impact Face C-scan of Impact Face Back Face C-scan of Back Face

a) 17-layered Satin Weave Laminate with 12.7-mm Grid (Panel2B, 113 m/s)

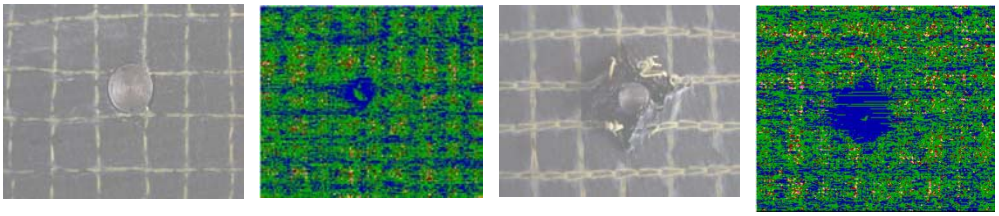

Impact Face C-scan of Impact Face Back Face C-scan of Back Face

b) 17-layered Satin Weave Laminate with 12.7-mm Grid (Panel 1B, 97 m/s)

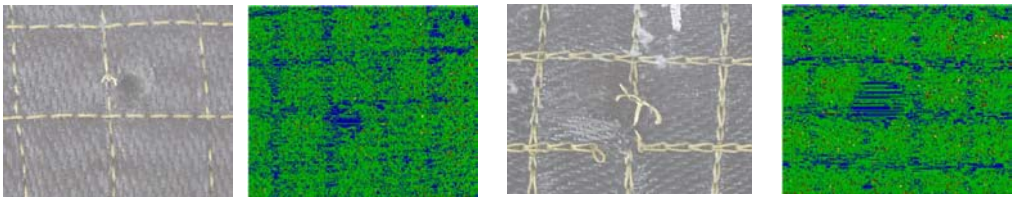

Impact Face C-scan of Impact Face Back Face C-scan of Back Face

c) 17-layered Satin Weave Laminate with 25.4-mm Grid (Panel 6D, 94 m/s)

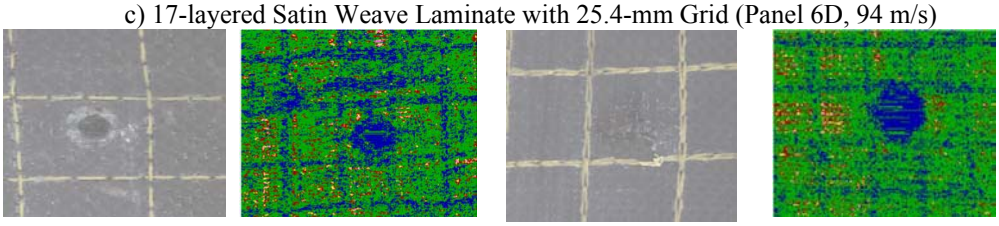

Impact Face C-scan of Impact Face Back Face C-scan of Back Face

d) 17-layered Satin Weave Laminate with 25.4-mm Grid (Panel 5D, 88 m/s)

Figure 19. Front and the Back Surface of 17-Layer Stitched Woven Carbon/Epoxy Samples Subjected to Ballistic Impact Loading with the Corresponding Ultrasonic C-Scan Images

laminates should be made based on whether the design requirement is improved damage tolerance or the ballistic limit.

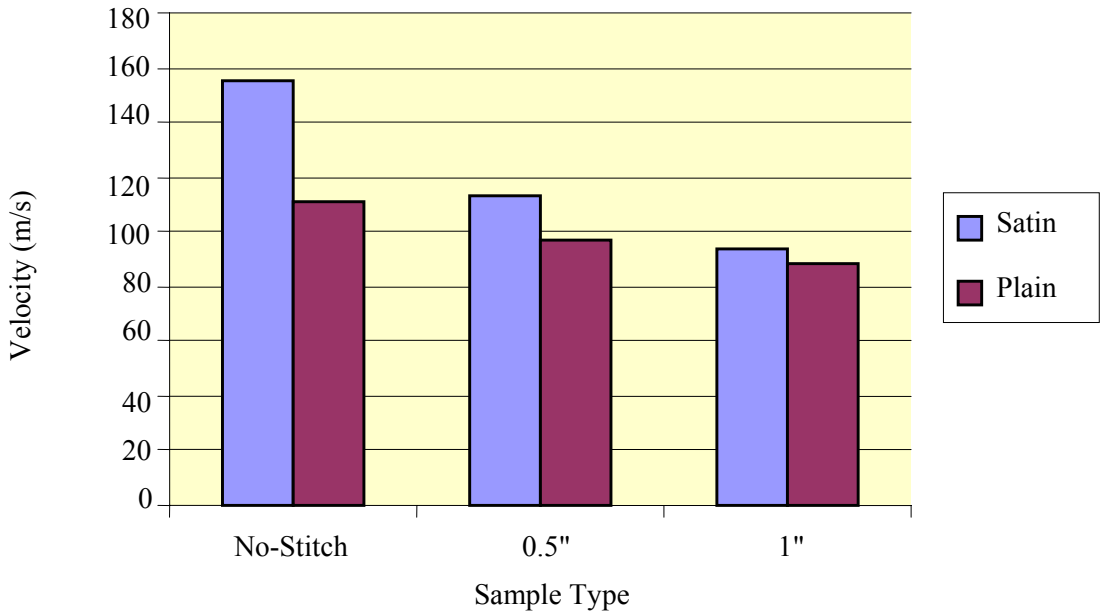

Figure 20. Comparison of Ballistic Limit for Different Laminate Configurations (17 layers)

Figure 21 a) and b) represent the comparison of the ballistic limits of satin and plain weave fabric stitched laminates for 12.7- and 25.4-mm stitch respectively. Ballistic limit is higher for satin weave laminates as compared to plain weave laminates. This could be attributed to the combined effect of two aspects. First, the thickness of satin weave laminates is relatively higher, which make them stiffer. The second reason is attributed to the the fabric architecture as already discussed in the previous section. The effect of fabric architecture is more pronounced in the case of 12.7 mm stitched samples, where the local effects play a dominant role. When the two thicknesses are compared, 17 layer laminates exhibit a higher ballistic limit than 7-layer laminates due to increased stiffness.

2.6 Effect of Projectile Shape on the Ballistic Perforation of VARTM Carbon/Epoxy Composite Panels

2.6.1 Introduction

In this part of the study, high-velocity impact tests were performed using a gas-gun test setup using four projectiles of different geometries (hemispherical, conical, fragment simulating, and flat tip; see Figure 22) each made from tool steel and weighing 14 g. Samples of dimension 101.6 by 101.6 mm (4 x 4 inches) were used. The sample was mounted in a simply supported boundary condition along its four edges, sandwiched on rollers between two rigid aluminum plates. Two chronographs (Model-ProChrono Digital) were mounted with clamps to the bottom of the capture chamber with a transparent optical window to record the incident and residual velocity of the projectile. Varying the pressure of gas in the firing chamber varied the impact velocity. The impact tests were designed to investigate the damage evolution at the ballistic limit. At least three samples were tested in each category to ensure repeatability. The ballistic limit velocity, $V_{BL,}$ and the resulting energy absorbed by each specimen are reported in Table 8.

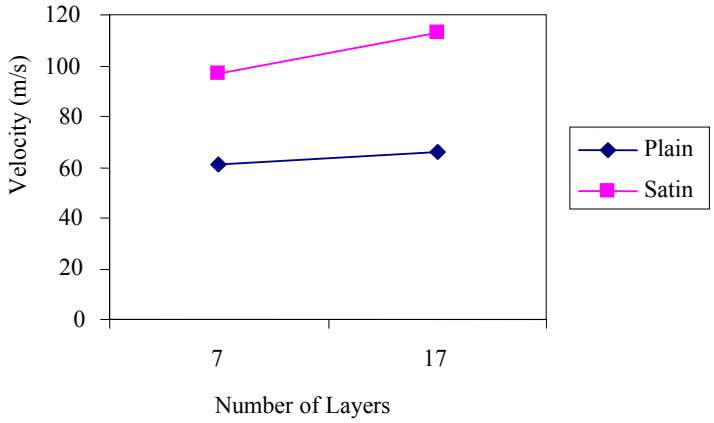

a)

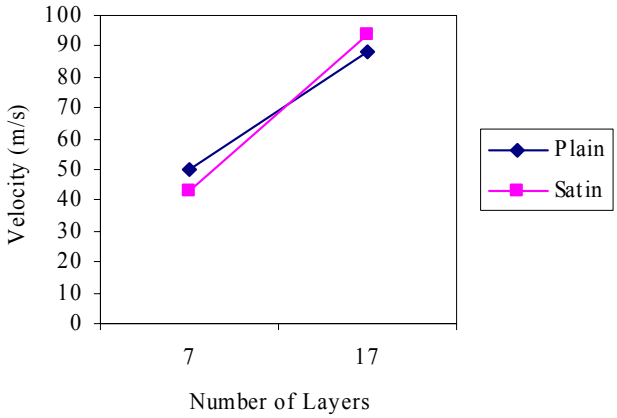

b)

Figure 21. Comparison of Ballistic Limits; a) 12.7-mm Grid, and b) 25.4-mm Grid

Table 8. Sample Number, Sample Thickness

Sample	Thickness (mm)
AC7	6.5
BC2	3.2
AF4	6.5
BF6	3.2
AH1	6.5
BH2	3.2
AFS2	6.5
BFS1	3.2

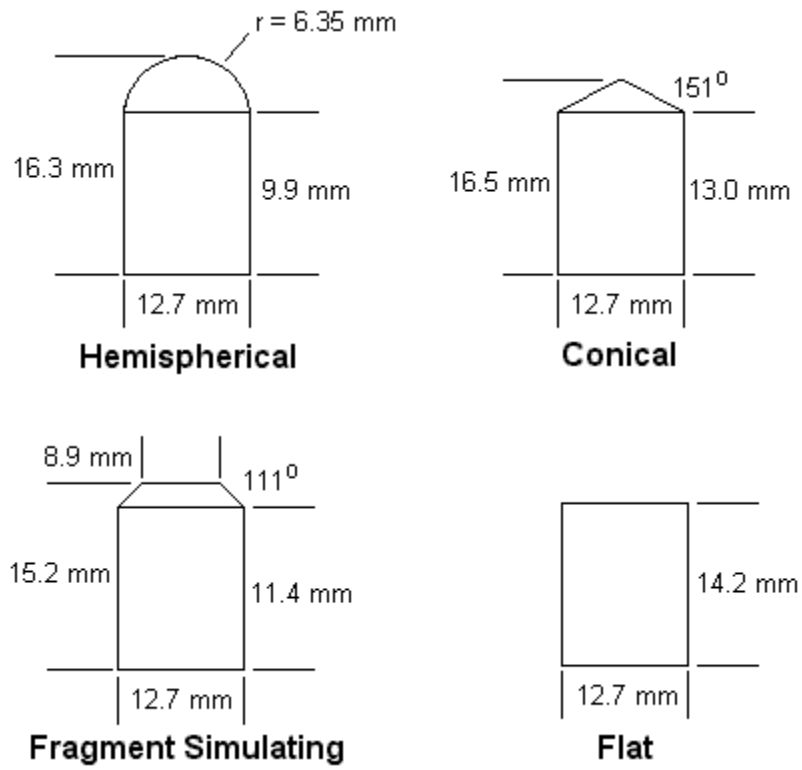

Figure 22. Projectile Shape and Dimensions

2.6.2 Specimen Fabrication

The composite panels were fabricated using eight-harness satin weave carbon fabric Style 5999 weighing 3.66 kg/m2 supplied by Fiber Materials Inc. and Applied Poleramic SC-15 epoxy resin-type through a VARIM. Two different thicknesses of composite panels were fabricated, one containing 7 layers (3.2 mm) and the other containing 17 layers (6.5 mm) of carbon fabric. The nomenclature (thickness, projectile shape, sample number) and resulting thickness of the panels are provided in Table 9.

Table 9. Sample Number, Velocity at Ballistic Limit, Energy Absorbed

Sample	Velocity at V_{BL} (m/s)	Energy (J)
AC7	167	195
BC2	90	57
AF4	155	168
BF6	91	58
AH1	153	164
BH2	79	44
AFS2	141	139
BFS1	77	42

Table 10. Sample Number, Average Transverse Crack Length, Average Longitudinal Crack Length

Sample	Avg. Trans. Crack (mm)	Avg. Long. Crack (mm)
AC7	31.6	16.6
BC2	17.7	15.5
AF4	23.5	15.3
BF6	20.5	20.6
AH1	21.6	19.1
BH2	15.8	15.2
AFS2	20.8	32.5
BFS1	15.1	16.3

2.6.3 Results and Discussion

2.6.3.1 Impact Testing

The samples exhibited transverse and longitudinal cracking patterns and these features were quantified. The incident velocity was measured for each specimen. The damage evaluation and assessment of failure modes of the target was carried out by measuring the parameters illustrated in Figure 23 with respect to the back face. Due to the variation in crack lengths from the center of penetration within each specimen, an average for half of the total transverse and longitudinal crack lengths was measured. These included both average transverse and average longitudinal crack growth. These measurements provided information about the principle dimensions of the impact damage zone such as entrance and exit areas for perforation and the damage profile (shape, size, and location). Table 10 summarizes the damage observations at V_{BL} for each specimen.

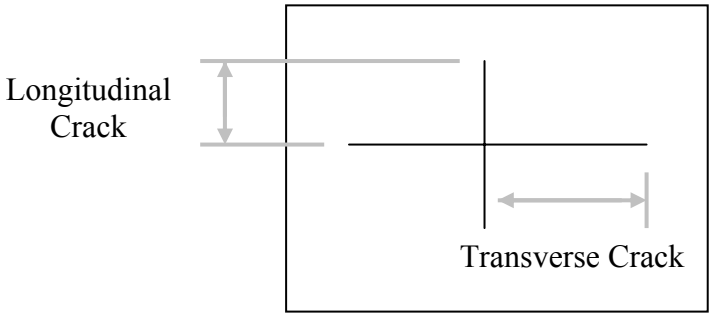

Figure 23. Quantitative Measurements on Back Face

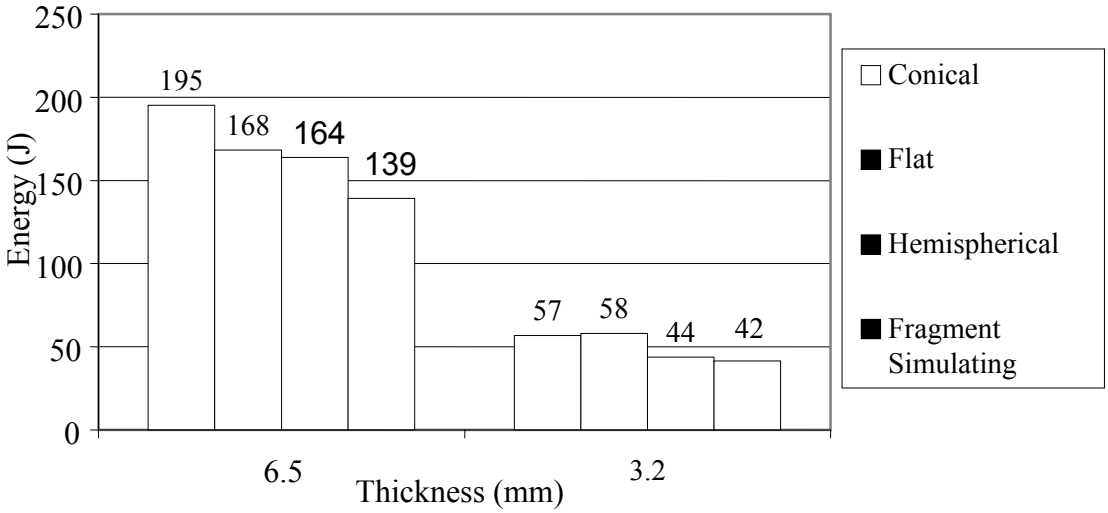

Figure 24 Energy Absorbed at Ballistic Limit Velocity for Each Specimen

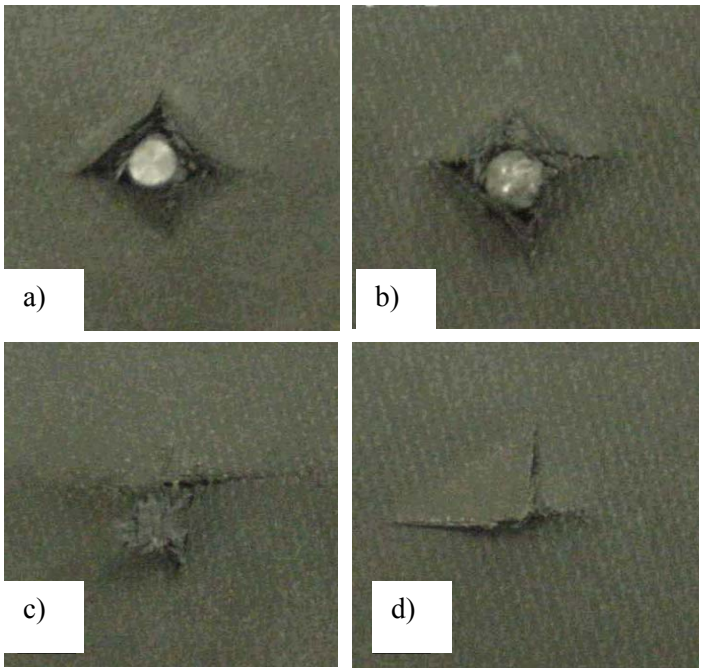

Figure 25. Back Face Damage of a) Fragment Simulating, b) Hemispherical, c) Conical, d) Flat Projectiles for 6.5-mm Thick Panels

Energy absorbed by each specimen at ballistic limit is represented in Figure 24. The influence of projectile geometry is seen to significantly affect the ballistic resistance of the panels. The influence of projectile geometry is more for the thicker specimens. In the 6.5-mm-thick specimens, the largest amount of energy absorbed in the panel occurred from the impact of the conical projectile (29 percent greater),

followed by the flat (17 percent greater), hemispherical (15 percent greater), and fragment simulating. The FSP penetrates with a lower velocity because it initially creates a small shear zone followed by elastic/plastic hole enlargement. The flat projectile also creates shear zone during impact, which results in plugging or ejection of a circular plug, but the energy absorbed is much greater due to the large impact face. Failure in the panels impacted with the conical and hemispherical projectiles resulted in elastic/plastic hole enlargement where the fibers are more likely to spread and stretch while the projectile penetrates (Figure 25). However, due to a small angle on the conical projectiles and the large surface area on the hemispherical projectiles, part of the failure is also a result of shear loading of the laminate.

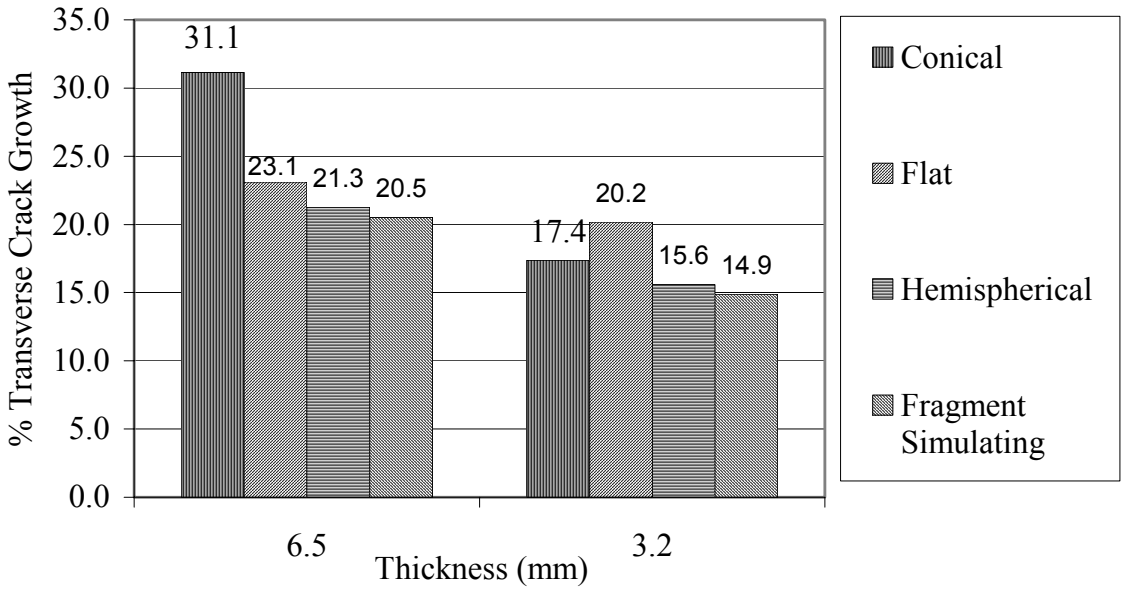

Figure 26. Average Transverse Crack Growth for Each Specimen

The average transverse crack growth correlates well with the type of failure that occurs in each panel. However, the average longitudinal crack growth in the panels did not vary as much under impact of the four different projectiles. The average transverse crack growth in the panels was the largest due to the impact of conical projectile (34 percent greater), followed by the flat (11 percent greater), hemispherical (4 percent greater), and FSP (Figure 26). The energy absorbed by each panel increases as the amount of cracking, due to back face tension, increases. Because of the difference in interlacing of the woven fibers in the warp and weft directions, the amount of energy absorbed in tension is more significant in the transverse direction than the longitudinal direction; thus, the cracking was more significant in the transverse than the longitudinal direction. Figure 2.6 illustrates the back face damage for the 6.5-mm panels.

In the 3.2-mm thick specimens, the range of energy absorbed is not as large, yet the amount of energy absorbed is higher for conical and flat than for the hemispherical and FSPs (average 25 percent greater, see Figure 24). The failure modes described above for the 6.5-mm-thick panels impacted with the four different projectiles are semicharacteristic of the 3.2 mm thick panels. The transverse and longitudinal crack growths also do not have a large range of values (~5 percent crack growth difference, Figure 26 and 27). The crack growth in the panels resulting from the impact of the conical and flat projectiles are slightly larger than the crack growth in the panels with hemispherical and the FSP impact, indicating the

absorption of energy is greater in the panels with longer cracks. Figure 28 illustrates the back face damage for the 3.2-mm panels.

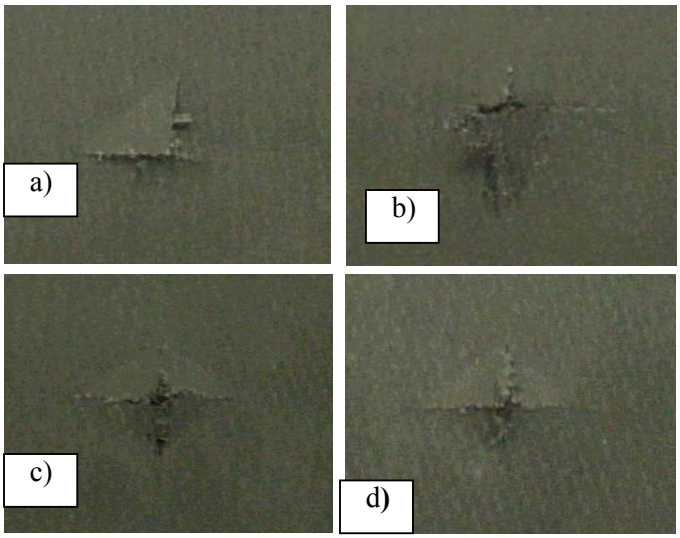

Figure 27. Back Face Damage of a) Fragment Simulating, b) Flat, c) Hemispherical, and d) Conical Projectiles for 3.2-mm Thick Panels

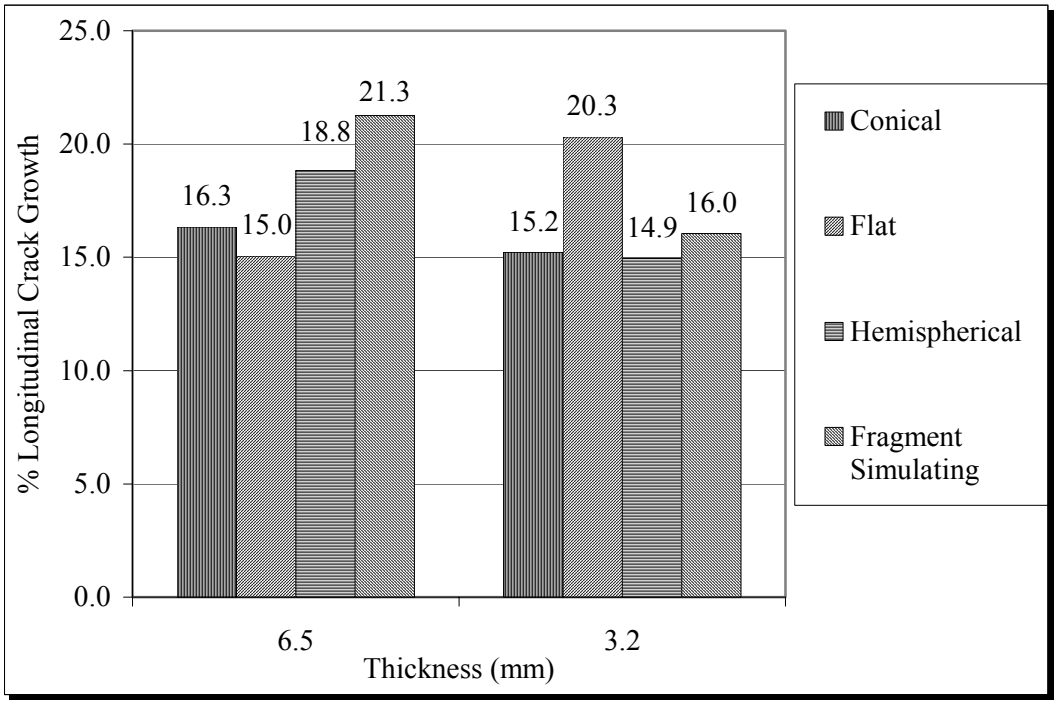

Figure 28. Average Longitudinal Crack Growth for Each Specimen

Due to the small variation in ballistic limit and crack propagation, penetration of carbon/epoxy panels by different-shaped projectiles is significantly dependent on panel thickness. Thin carbon/epoxy panels flex readily during the ballistic event which absorbs a majority of the projectiles energy regardless of shape.

2.7 Analytical Modeling

Wen's analytical models [17, 18] were used for the prediction of ballistic limit in each panel impacted by the four different projectiles. The following equations were derived from energy relationships. Each equation is specific to the shape of projectile. The parameters for the equations are also listed.

Conical

$$V_{BL} = \frac{\pi \sin\left(\frac{\theta}{2}\right)\sqrt{\rho_t \sigma_e} D^2 T}{2G}\left[1 + \sqrt{1 + \frac{2G}{\pi \sin^2 \frac{\theta}{2} \rho_t D^2 T}}\right] \tag{1}$$

Hemispherical

$$V_{BL} = \frac{3\pi\sqrt{\rho_t \sigma_e} D^2 T}{8G}\left[1 + \sqrt{1 + \frac{32G}{9\pi \rho_t D^2 T}}\right] \tag{2}$$

Flat

$$V_{BL} = \frac{\pi\sqrt{\rho_t \sigma_e} D^2 T}{2G}\left[1 + \sqrt{1 + \frac{2G}{\pi \rho_t D^2 T}}\right] \tag{3}$$

Fragment Simulating

$$V_{BL} = \sqrt{\frac{2\pi a^2 T \sigma_{cone}}{G}}\left[1 + \left(\frac{\sigma_{flat}}{\sigma_{cone}} - 1\right)\left(\frac{a_T}{a}\right)^2\right]^{\frac{1}{2}} \tag{4}$$

The parameters for the predictive ballistic limit equations are as follows:

- a projectile radius
- a_T radius of tapered section for a FSP
- D projectile diameter
- G projectile mass
- T thickness of laminate
- V_{BL} ballistic limit of the laminate
- θ cone angle of conical projectile
- ρ_t density of the laminate

- σ_e elastic limit of the laminate in through-thickness compression
- σ_{flat} mean pressure of the laminate to resist a flat projectile
- σ_{cone} mean pressure of the laminate to resist a conical projectile

Sample calculation for the prediction of hemispherical projectile ballistic limit velocity in the thick (6.5 mm) panel follows:

$$V_{BL} = \frac{3\pi\sqrt{\rho_t \sigma_e} D^2 T}{8G}\left[1+\sqrt{1+\frac{32G}{9\pi\rho_t D^2 T}}\right] \tag{5}$$

D = 0.0127 m, G = 0.014 kg, T = 0.0065 m, ρ_t = 1550 kg/m^3, σe = 211 MPa

$$V_{BL} = \frac{3*\pi*\sqrt{1550*211}*(0.0127)^2*0.0065}{8*0.014}\left[1+\sqrt{1+\frac{32*0.014}{9*\pi*1550*(0.0127)^2*0.0065}}\right] \tag{6}$$

$$V_{BL} = 216\, {}^{m}\!/_{s} \tag{7}$$

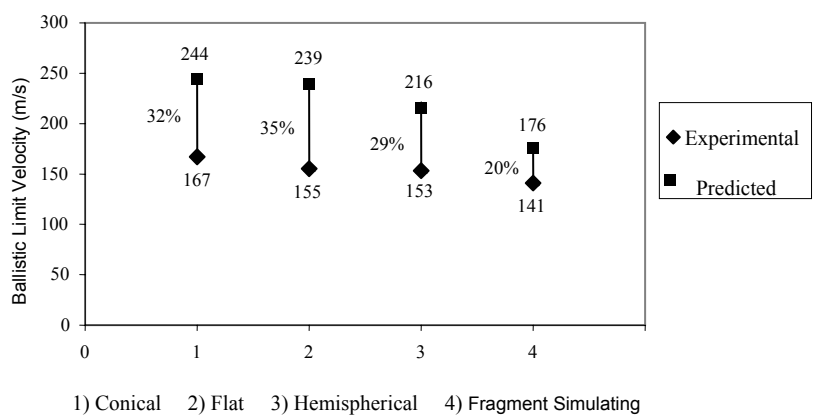

Figure 29. Predicted and Experimental Ballistic Limit Velocity for the 6.5-mm Thick Panels

The predictions calculated from the models follow the general trend of the experimental results for 6.5- and 3.2-mm-thick laminates (see Figure 29 and 30, in which the number on the x-axis corresponds to the type of projectile). However, the models overestimate the ballistic limit by as much as 35 percent for the 6.5-mm panels and 43 percent for the 3.2-mm panels. The difference in magnitude between the models and the experiments is attributed to three factors-failure mechanisms, weave architecture (for example, plain versus satin weave) within the woven carbon/epoxy panels, and the boundary condition (clamped versus simply supported). Due to the difference in interlacing of the woven fibers in the warp and weft directions, the amount of energy absorbed in tension varies. The shearing caused by the crimping and undulations of the fabric decreases the ballistic limit. The elastic limit of the laminates in through-

thickness compression also needs to be better understood for the studied carbon/epoxy panels in order to more closely predict the ballistic limit for each projectile shape. The trends of the experiment, though, follow the model accurately.

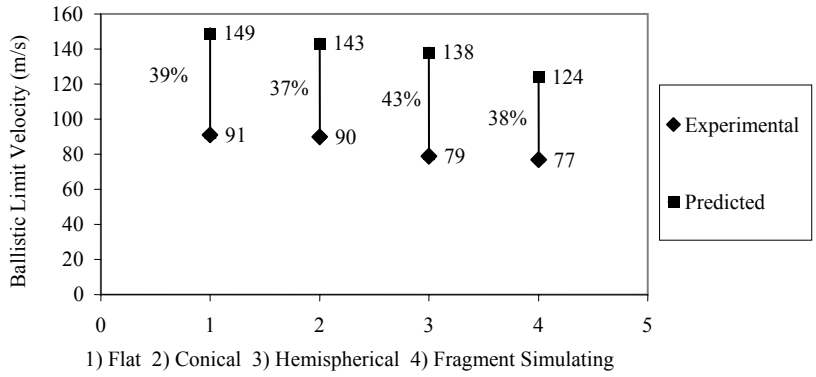

Figure 30. Predicted and Experimental Ballistic Limit Velocity for the 3.2-mm Thick Panels

2.8 Summary

2.8.1 Studies on Plain and Twill Weave Samples with Polycarbonate Facing

- Woven carbon fabric composites of plain, 2/2 twill, and hybrid weaves manufactured by the VARTM process and bonded to polycarbonate facing were subjected to ballistic impact under simply supported boundary condition. The role of the sacrificial polycarbonate facing was to reduce the incident velocity of impact to the panel and withstand low velocity impact.
- The twill weave panels exhibited 20 percent higher ballistic limit than the plain weave. The hybrid weave exhibited a ballistic response in between that of the plain and satin weave and was sensitive to the positioning of the weave with respect to the impact direction.
- The progression of damage and damage modes were found to be sensitive to the position of the plies and the type of woven fabric. The prominent damage modes were tensile side fracture of the plies for 2/2 twill weave dominant samples, and fiber shear fracture for the plain weave dominate samples.

2.8.2 Studies on Stitched/Unstitched Plain and Satin Weave Laminates

- 7-, 17- and 37-layer woven carbon fabric composites of plain and satin weave were subjected to ballistic impact loading to determine the ballistic limit.
- Ballistic limit for satin weave was about 38 percent higher than plain weave laminates for 7- and 17-layer samples and about 13 percent higher for thick panels (37 layers).
- There was more damage area in satin weave laminates, which showed predominant flexural tensile failure as compared to the dominant shear failure mode in plain weave laminates.
- The architecture of the weave did not play as large of a role (in terms of ballistic limit) in the thin samples as opposed to the thicker samples.
- In the thick samples, it was very apparent that the satin weave absorbed more ballistic energy than the plain weave.

- In the thin samples with the 12.7-mm grid, the point of impact became very significant. If the FSP impacted the sample on a stitch (eg. 8C), the damage was considerably larger than if the FSP impacted between stitches (eg. 7D). This may be due to the inability of the sample to flex because of a high stitch density.
- In the 25.4-mm grid, we did not see as large a difference, whether the FSP impacted the sample at a stitch or between stitches. In general,
    - Ballistic limit trends - unstitched > stitched with 12.7 mm grid > stitched with 25.4 mm grid
    - Unstitched ballistic limit ~ 37 percent higher with respect to. 12.7-mm grid stitched samples
    - Unstitched ballistic limit ~ 59 percent higher with respect to 25.4-mm grid stitched samples.
- The samples with the 0.5-inch grid did perform better than the samples with the 1-inch grid when the FSP impacted at a stitch.

2.8.3 Influence of Projectile Shapes

- The influence of projectile shape in the studied carbon/epoxy laminates under high-velocity impact resulted in a range of energy absorption at ballistic limit: conical > flat > hemispherical > FSP.
- Failure mechanisms of plugging, separation of fibers, or a combination of both are a result from the high-velocity impact of different-shaped projectiles on the carbon/epoxy laminates studied.
- Panel thickness has a significant effect on the ballistic limit of panels impacted by different-shaped projectiles. Thin carbon/epoxy panels bend easily during a ballistic event, which absorbs a majority of the projectiles energy regardless of shape. In thick carbon / epoxy panels, projectile shape induces different failure mechanisms, which result in different ballistic limits.
- The trend of ballistic limits for the carbon/epoxy laminates impacted by different-shaped projectiles was predicted using current analytical equations.

3. References

1. Mallick, P. K., "Fiber Reinforced Composites," Second Edition, Marcel Dekker Inc., New York, USA (1993).
2. Abrate, S., "Impact to Composite Structures," Cambridge University Press, Cambridge, UK (1998).
3. Zukas, J. A., and Scheffler, D. R., "Impact Effects in Multilayered Plates," *International Journal of Solids and Structures*, Vol. 38, No. 19, pp. 3321-3328, (2001).
4. Wang, B., and Lu, G., "On the Optimization of Two Component Plates Against Ballistic Impact, *Journal of Materials Processing Technology,* Vol. 57, pp. 141-145, (1996).
5. Hetherington. J. G., and Rajagopalan, B. P., "An Investigation Into the Energy Absorbed During Ballistic Perforation of Composite Armours, *International Journal of Impact Engineering,* Vol. 11, No. 1, pp. 33-40, (1991).
6. Wilkins, M. L., "Mechanics of Penetration and Perforation," *International Journal of Engineering Science,* 16, pp.793-807, (1978).
7. Bless, S. J., and Hartman, D. R., "Ballistic Penetration of S-2 Glass Laminates," *Proc. 21st International SAMPE Technical Conference, 21,* pp. 852-856, (1989).
8. Ng, S., Tse, P., and Lau, K., "Numerical and Experimental Determination of In-Plane Elastic Properties of 2/2 Twill Weave Fabric Composites," *Composites Part B: Engineering,* Vol. 29, No. 6, pp. 735-744, (1998).
9. Bersuch, L., Benson, R., and Owens, S., Affordable Composite Structure for Next Generation Fighters, *Society for the Advancement of Materials and Process Engineering, Materials and Process Affordability: Keys to the Future,* 43, pp. 56-65, (1998).
10. Taylor, A., "RTM Material Developments for Improved Processability and Performance," *SAMPE Journal,* Vol. 36, No. 4, (July/August 2000).
11. Faiz, R., "Net RTM Preforming Process for Cost Effective Manufacturing of Military Ground Vehicle Composite Structures," *Proc. 28th Int. SAMPE Symp.,* pp. 381-292, (1996).
12. Schwartz, M. M. "Composite Materials - Processing, Fabrication and Applications," Prentice-Hall Publishers, Vol. II (1996).
13. Scida, D., Aboura, Z., Benzeggagh, M. L., and Bocherens E., "A Micromechanics Model for 3D Elasticity and Failure of Woven-Fibre Composite Materials," *Composites Science and Technology,* Vol. 59, No. 4, pp. 505-517, (1999).
14. Scida, D., Aboura, Z., Benzeggagh, M. L., and Bocherens E., "Prediction of the Elastic Behaviour of Hybrid and Non-Hybrid Woven Composites," *Composites Science and Technology*, Vol. 57, No. 12, pp.1727-1740, (1998).
15. Naik, N. K., and Ganesh V. K., "Prediction of On-Axes Elastic Properties of Plain Weave Fabric Composites," *Composites Science and Technology,* Vol. 45, No. 2, pp. 35-152, (1992).
16. Vaidya, U. K., Kulkarni, M., Haque, A., Hosur, M. V., and Kulkarni, R., "Ballistic Performance of Graphite/Epoxy and S2-Glass/Epoxy Composites With Polycarbonate Facing," *Materials Technology,* Vol. 15, No.3, pp.202-214, (2000).
17. Wen, H. M., "Predicting the Penetration and Perforation of FRP Laminates Struck Normally by Projectiles with Different Nose Shapes," *Composite Structures,* Vol. 49, No. 3, pp. 321-329, (2000).
18. Wen, H. M., "Penetration and perforation of thick FRP laminates," *Composites Science and Technology,* Vol. 61, pp. 1163-1172, (2001).
19. Ben-Dor, G., Dubinsky, A., and Elperin, T., "Optimal Nose Geometry of the Impactor Against FRP Plates," *Composite Structures,* Vol. 55, No. 1, pp. 73-80, (2002).
20. Ben-Dor, G., Dubinsky, A., and Elperin, T., "A Model for Predicting Penetration and Perforation of FRP Laminates by 3-D Impactors," *Composite Structures*, Vol. 56, No. 3, pp. 243-248, (2002).

21. Gellert, E. P., Cimpoeru, S. J., and Woodward, R. L., "A Study of the Effect of Target Thickness on the Ballistic Perforation of Glass-Fibre-Reinforced Plastic Composites," *International Journal of Impact Engineering*, Vol. 24, No. 5, pp. 445-456, (2000).
22. Lee, S. W. R, Sun, C. T., "Dynamic Penetration of Graphite/Epoxy Laminates Impacted by a Blunt-Ended Projectile," *Composites Science and Technology,* Vol. 49, No. 4, pp. 369-380, (1993).
23. Huang, S.L., Richey, R. J., and Deska, E.W., "Cross-Reinforcement in a GFRP Laminate," Paper presented at ASME, Winter Annual meeting, San Francisco, USA, (1978).
24. Mignery, L. A., Sun, C. T., and Tan, T. M., "The Use of Stitching to Suppress Delamination in Laminated Composites," *ASTM STP 876,* pp. 371-385, (1985).
25. Kang, T. J., and Lee. S. H., "Effect of Stitching on the Mechanical and Impact Properties of Woven Laminate Composite," *Journal of Composite Materials,* Vol. 28, No. 16, pp. 1574-1587, (1994).
26. Dransfield, K., Baillie, C., and Mai, Y. M., "Improving the Delamination Resistance of CFRP by Stitching – Review," Composites Science & Technology, Vol. 50, No. 3, pp. 305-317 (1994).
27. Mouritz, A. P., and Cox, B. N., "A Mechanistic Approach to the Properties of Stitched Laminates," *Composites Part A: Applied Science and Manufacturing,* Vol. 31, No. 1, pp. 1-27, (2000).
28. Mouritz, A. P, Leong, K. H., and Herszberg, I., Composites *Part A: Applied Science and Manufacturing,* 28, pp. No. 12, 979-991(1997).
29. Su, K. B., "Delamination Resistance of Stitched Thermoplastic Matrix Composite Laminates," *ASTM STP 1044,* pp. 279–300(1989).
30. Jain, L. K., and Mai, Y. W. 1995. "Determination of Mode II Delamination Toughness of Stitched Laminated Composites," Composites Science and Technology, Vol. 55, No. 3., 241-253
31. Shu, D. W. Mai, Y. W. "Effect of Stitching on Interlaminar Delamination Extension in Composite Laminates," *Composites Science and Technology,* Vol. 49, No. 2, 165-171
32. Farley, G. L., Smith, B. T., and Maiden, J., "Compression Response of Thick Layer Composite Laminates With Through-The-Thickness Reinforcement," *Journal of Reinforced Plastics and Composites* Vol. 11, pp. 787–810, (1992).
33. Liu, D. "Delamination Resistance in Stitched and Unstitched Composite Planes Subjected to Composite Loading," *Journal of Reinforced Plastics and Composites,* Vol. 9, No. 1, 59-69
34. Pelstring, R. M., and Madan, R.C., Stitching to Improve Damage Tolerance of Composites. In: *Proc. 24th Int. SAMPE Symp.,* pp. 1519–1529, (8–11 May 1989).
35. Dexter, H. B., "Innovative Textile Reinforced Composite Materials for Aircraft Structures," *SAMPE Journal,* Vol. 28, pp. 404-416 (1996).

4. Bibliography

Published/Inprint (Journals)

1. Hosur, M. V., Vaidya U. K., Ulven, C., and Jeelani S., **"**Performance of Stitched/Unstitched Woven Carbon/Epoxy Composites Under High Velocity Impact Loading," *Composite Structures* (in print)
2. Hosur, M. V., Alexander, J., Vaidya, U. K., Mayer, A., Jeelani, S., "Studies on the off-axis high strain rate compression loading of satin weave carbon/epoxy composites," *Composite Structures* Vol. 63, No. 1,2004 pp. 75-85.
3. Hosur, M. V., Adya, M., Alexander, J., Vaidya, U. K., Mayer, A., and Jeelani, S., "Studies on Impact damage Resistance of affordable Stitched woven Carbon/Epoxy Composite Laminates," *Journal of Reinforced Plastics and Composites,* Vol. 22, No. 10, 2003, pp. 927-952.
4. Hosur, M. V., Alexander, J., Vaidya, U. K., Mayer, A., Jeelani, S., "High Strain Rate Compression Characterization of Plain Weave Carbon/Epoxy Composites under off-axis loading," *Polymers and Polymer Composites*, Vol. 11, No. 7, 2003, 527-540.
5. Vaidya, U. K., Ulven, C., Hosur, M. V., Alexander, J., and Liudahl, L., "Ballistic Impact Study on Woven Carbon/Epoxy Composites with Polycarbonate Facing," *Polymers and Polymer Composites*, Vol. 11, No. 6, 2003, pp. 421-432.
6. Ulven, C., Vaidya, U. K., and Hosur, M. V., "Effect of Projectile Shape During Ballistic Perforation of VARTM Carbon/Epoxy Composite Panels," *Composite Structures,* 61, No. 1-2, 2003, pp. 143-150.
7. Hosur, M. V., Adya, M., Vaidya, U. K., Mayer, A., and Jeelani, S., "Effect of Stitching and Weave Architecture on the High Strain Rate Compression Response of Affordable Woven Carbon/Epoxy Composites" *Composite Structures,* Vol. 59, No. 4, 2003, pp. 507-523.
8. Hosur, M. V., Alexander, J., Vaidya, U. K., Mayer, A., Jeelani, S., "High Strain Rate Compression Response of Affordable Woven Carbon/Epoxy Composites," *Journal of Reinforced Plastics and Composites,* Vol. 22, No. 3, 2003, pp. 271-296.
9. Hosur, M. V., Alexander, J., Vaidya, U. K., Jeelani, S., "High Strain Rate Compression Response of Carbon/Epoxy Laminate Composites," *Composite Structures,* Vol. 52, No. 3-4, 2001, 405-417.

Under Preparation (Journal)

1. Nwosu, S., and Ali-Al-Quraishi, "Quantitative analysis of perforated carbon-epoxy plates by Micro-Raman Spectroscopy."
2. Nwosu, S., Blemann, R., and Mayer A., "Determination of perforation threshold velocity using integrative penetrating Hopkinson bar system."
3. Nwosu, S., "Energy absorbed profiling using dynamic optical imaging of high-speed digital video camera."
4. Nwosu, S., Ojo, F., Slaughter, W., and Hosur, M., "The effects of Projectile Geometry on the Damage Response of Woven Graphite/Epoxy composite."

Conference Proceedings/Presentations

1. Kelkar. A. D., Tate, J. S., and Bolick, R., "Post Impact Fatigue Behavior of Low Cost VARTM Manufactured Woven Composite Laminates," 35th SAMPE meeting, Dayton, OH, September 2003.
2. Kelkar A. D., Tate, J. S., and Bolick, R., "Introduction To Low Cost Manufacturing of Composite Laminates," to appear in the proceedings of the ASEE Annual Conference (Paper #1482), Nashville, TN, June 2003.
3. Hosur, M. V., Vaidya, U. K., Ulven, C., Mayer, A., and Jeelani, S., "Ballistic Impact Response of Woven Carbon/Epoxy Composites," SAMPE 2003, May 11-15, 2003, Long Beach, CA.

4. Kelkar, A. D., and Tate, J. S., "Low Cost Manufacturing of Textile Composites Using Vacuum Assisted Resin Transfer Molding," Proceedings of the 20th All India Manufacturing Technology, Design and Research Conference, December 2002, Ranchi, India, p712-716.
5. Hosur, M. V., Adya, M., Vaidya, U. K., and Jeelani, S., "Response of Stitched Woven Carbon/Epoxy Composites Under High Strain Rate Compression Loading," SAMPE Technical Conference, November 4-7, 2002, Baltimore, MD.
6. Ulven, C., Vaidya, U. K., and Hosur, M. V., "Effect of Projectile Shape during Ballistic Perforation of VARTM Carbon/Epoxy Composite Panels," SAMPE Technical Conference, November 4-7, 2002, Baltimore, MD.
7. Kelkar, A. D., "Behavior of Thin, Moderately Thick and Thick Woven Composites Subjected to Low Velocity Impact Loads," Recent Advances in Solids and Structures, Proceedings of the ASME International Mechanical Engineering Congress And Exposition, New Orleans, November 2002.
8. Hosur, M.V., Alexander, J., Vaidya, U. K., Mayer, A., and Jeelani, S., "On and Off-Axis High Strain Rate Compression Characterization of Affordable Woven Carbon/Epoxy Composites," Proceedings of the 17th Annual Technical Conference of the American Society for Composites, Purdue, IL, October 20-23, 2002.
9. Vaidya, U. K., Ricks, H., and Ulven, C., "Vibration Testing of VARTM Processed Carbon/Epoxy Plates," International Congress on Acoustics and Vibration, Orlando, FL, July 2002 (IIAV website).
10. Vaidya, U. K., Ulven, C., and Hosur, M. V., "Ballistic Impact Study on Woven Carbon/Epoxy Composites," USNCTAM14, June 23-28, 2002, Blacksburg, VA.
11. Hosur, M. V., Alexander, J., Vaidya, U. K., and Jeelani, S., "Characterization Of Affordable Satin Weave Carbon/Epoxy Laminate Composites Under Dynamic Compression Loading," Southeastern Conference on Theoretical and Applied Mechanics, SECTAM XXI, May 19-21, 2002, Orlando, FL.
12. Kelkar, A. D., and Williams, A., "Aircraft Survivability of Affordable Composites," Proceedings of the 43rd AIAA /ASME/ ASCE/ AHS/ ASC Structures, Structural Dynamics, and Materials Conference, Denver, CO, April 2002 AIAA Paper 2002-1616.
13. Hosur, M. V., Adya, M., and Vaidya, U. K.,"Impact Resistance of Stitched Affordable Woven Carbon/Epoxy Composites," ASME International Mechanical Engineering Congress and Exposition, New York, NY, November 2001.
14. Vaidya U. K., and Ulven. C., "Ballistic Impact Response of Hybridized Carbon/Epoxy VARTM Composites," 31st SAMPE Technical Conference, Seattle, Nov. 2001.
15. Hosur, M. V., Alexander, J., Vaidya U. K., and Jeelani, S., "Off-Axis High Strain Compression Response of Carbon/Epoxy Laminates," Proceedings of the 16th Annual Technical Conference of the American Society for Composites, Blacksburg, VA, September 9-12, 2001.
16. Hosur, M. V., Adya, M., Vadiya, U.K., Mayer, A., and Jeelani, S., "Characterization of Affordable Stitched Plain Weave Carbon/Epoxy Composites Under Impact Loading," ICCM-13, Thirteenth International Conference on Composite Materials, June 25-29, 2001, Beijing, China.
17. Pai, D. M. and Kelkar, A. D., "Introduction to Low-Cost Manufacturing of Polymeric Composites," Proceedings of the ASEE Annual Conference (Paper #0844), Albuquerque, NM, June 2001.
18. Hosur, M. V., Alexander, J., Adya, M., Vaidya, U. K., and Jeelani, S., "Impact Response of Affordable Graphite/Epoxy Woven Fabric Composites," 42nd AIAA/ASME/ASCE/ASC Structures, Structural Dynamics and Materials Conference, Seattle, WA, 16-19 April, 2001.
19. Hosur, M. V., Alexander, J., Jeelani S., and Vaidya, U. K., "High Strain Rate Compression Response of Carbon/Epoxy Laminate Composites," ASME International Mechanical Engineering Congress and Exposition, Orlando, FL, November, 2000.
20. Hosur, M. V., Alexander, J., Vaidya U. K., and Jeelani, S., "High Strain Rate Response of Affordable Woven Graphite/Epoxy Composite Laminates," 7th International Conference on Composites Engineering, ICCE/7, Denver, CO, USA July 2-8, 2000.

Student Conference Presentations/Awards

1. Ulven C. A., and Vaidya, U. K., "Modal and Harmonic Analysis of Plain-Woven Carbon Fiber/Epoxy Composite Beams," University of Alabama at Birmingham (UAB) Graduate Student Research Day, Birmingham, AL, March 21, 2003.
2. Adya, M., "High Strain Compression Response Of Affordable Satin Weave Carbon/Epoxy Composites," 41st AIAA Aerospace Sciences Meeting and Exhibit Reno, Nevada, 6–9 January 2003.
3. Adya, M., "High Strain Compression Response Of Affordable Satin Weave Carbon/Epoxy Composites," Awarded First Place at the 2002 Southeastern Regional AIAA Student Paper Competition, Huntsville, Alabama, April 2002.
4. Adya, M., Hosur, M.V., "Dynamic Characterization of Stitched Woven Graphite/Epoxy Composites," 2002 Symposium on Experimental Mechanics, University Of Florida, Florida, March 2002.
5. M. Adya, M.V. Hosur "Response of Stitched Plain Weave Carbon/Epoxy Composites Under Low Velocity Impact," 52nd AIAA Southeastern Regional Student Conference, Atlanta, Georgia, April 2001.
6. Adya, M., Hosur, M.V., "Effect of Stitching on Carbon Composites," Awarded Second Place at Sigma Xi 28th Annual Student Research Symposium, Tuskegee University, Alabama, March 2001.
7. Alexander, J., "High Strain Rate Compression Response of Uni-directional Carbon/epoxy Laminate Composites - Effect of Fiber Orientation," presented (oral) at the Sigma Xi 28th Annual Student Research Symposium, Tuskegee University, AL, March 23-24, 2001(Won First Prize).
8. Alexander, J., "Failure of Woven Carbon/epoxy Laminate Composites Under Dynamic Compression Loading," presented (poster) at the Sigma Xi 28th Annual Student Research Symposium, Tuskegee University, AL, March 23-24, 2001 (Won First Prize).
9. Alexander, J., "High Strain Rate Response of Affordable Woven Graphite/Epoxy Composite Laminates," presented at the ASME student's competition of Chattahoochee section, Auburn University, AL, August 28, 2000 (Won Third Prize).

List of Acronyms

Acronym	Description
CAI	composite affordability initiative
CFRP	carbon fiber reinforced plastic
FATE	future aircraft technology enhancement
FSP	fragment simulating projectile
GRP	glass-reinforced plastic
LO	low observable
NCA&T	North Carolina A & T University
NDE	nondestructive evaluation
NDSU	North Dakota State University
RTM	resin transfer molding
TAFT	Today's Aircraft Flying Tomorrow
TU	Tuskegee University
UAB	The University of Alabama at Birmingham
UP	University of Pittsburgh
VARIM	vacuum-assisted resin infusion molding
VARTM	vacuum-assisted resin transfer molding